EFFECT OF TiH_2 PARTICLE SIZE ON FOAMING OF ALUMINIUM

A THESIS SUBMITTED TO
THE GRADUATE SCHOOL OF NATURAL AND APPLIED SCIENCES
OF
MIDDLE EAST TECHNICAL UNIVERSITY

BY

CEYLAN KUBİLAY

IN PARTIAL FULFILLMENT OF THE REQUIREMENTS
FOR
THE DEGREE OF MASTER OF SCIENCE
IN
METALLURGICAL AND MATERIALS ENGINEERING

DECEMBER 2005

Approval of the Graduate School of Natural and Applied Sciences

Prof. Dr. Canan ÖZGEN
Director

I certify that this thesis satisfies all the requirements as a thesis for the degree of Master of Science.

Prof. Dr. Tayfur ÖZTÜRK
Head of Department

This is to certify that we have read this thesis and that in our opinion it is fully adequate, in scope and quality, as a thesis for the degree of Master of Science.

Prof. Dr. Tayfur ÖZTÜRK
Supervisor

Examining Commitee Members

Prof.Dr. Şakir Bor _____

Prof.Dr. Tayfur Öztürk _____

Prof.Dr.Engin Kılıç _____

Prof.Dr. Vedat Akdeniz _____

Assoc.Prof.Dr.Kadri Aydınol _____

I hereby declare that all information in this document has been obtained and presented in accordance with academic rules and ethical conduct. I also declare that, as required by these rules and conduct, I have fully cited and referenced all material and results that are not original to this work.

Ceylan KUBİLAY

ABSTRACT

EFFECT OF TiH_2 PARTICLE SIZE ON FOAMING OF ALUMINIUM

Kubilay, Ceylan

M.S., Department of Metallurgical and Materials Engineering

Supervisor: Prof. Dr. Tayfur Öztürk

December 2005, 47 pages

A study is carried out on the production of aluminum foams via powder processing. The study deals mainly with the effect of TiH_2 particle size on the process of foaming. Mainly two TiH_2 particle sizes were used; namely 27,5 μm and 8,5 μm. Foaming experiments were carried out at temperatures between 675°C – 840°C. The viscosity of the system is adjusted by controlled addition of Al_2O_3. The study shows that choice of foaming agent size is influential in the foaming process. With the use of fine foaming agent, temperatures in excess of 800°C would be required for successful foaming. The study further showed that the relation between foaming and viscosity was also dependent on the particle size. Viscosity of 2.3 mPa.s was found to be a limiting value for successful foaming with fine foaming agent. This value appears to increase with increasing particle size. An analysis is presented with regard to temperature dependence of foaming, which takes into account the effect of particle size.

Keywords: Aluminium Foam, Minimum Critical Particle Size, Viscosity, Pore Nucleation, TiH_2.

ÖZ

ALÜMİNYUM KÖPÜKLERDE TiH_2 PARÇACIK BOYUTUNUN KÖPÜRMEYE ETKİSİ

Kubilay, Ceylan

Y.Lisans., Metalurji ve Malzeme Mühendisliği Bölümü

Tez Yöneticisi: Prof. Dr. Tayfur Öztürk

Aralık 2005, 47 sayfa

Bu çalışma alüminyum köpüklerin toz metalurjisi yöntemleri ile üretimini konu almaktadır. Çalışma ana olarak köpürtücü tane büyüklüğünün (TiH_2) köpürme sürecine etkisini farklı sıcaklık ve viskozite değerlerinde ele almaktadır. Bu amaçla 27,5 ve 8,5 μm büyüklüğünde iki farklı boyutta TiH_2 köpürtücü kullanılmış ve köpürme 675^oC – 840^oC aralığında incelenmiştir. Viskozite kontrolü sisteme Al_2O_3 ilavesi ile gerçekleştirilmiştir. Yapılan çalışma köpürmenin köpürtücü büyüklüğüne bağlı olduğunu, ince köpürtücü kullanımı durumunda makul köpürme için 800^oC ve üstü sıcaklıkların gerekli olduğunu göstermiştir. Ayrıca çalışma, köpürme-viskozite ilişkisinde köpürtücü büyüklüğünün etkili olduğunu, ince köpürtücü kullanımı durumunda 2,3 mPa.s üstü viskozitelerde köpürme olmazken, iri köpürtücü kullanımı durumunda bu değerin daha yüksek olduğunu göstermiştir. Köpürme süreci, köpürtücü tane büyüklüğüne bağlılık temelinde irdelenmiş ve köpük hücrelerinin çekirdeklenmesinde etkin bir minimum tane büyüklüğünün gerekli olduğu gösterilmiştir.

Anahtar kelimeler: Alüminyum Köpük, Minimum Köpürtücü Tane Büyüklüğü, Viskozite, Gözenek Çekirdeklenmesi, TiH_2.

To My Family

ACKNOWLEDGEMENTS

I am grateful to Prof.Dr.Tayfur Öztürk for his advice and support throughout the entire period of the study. Thanks are due to Prof. Dr. Bilgehan Ögel and Prof. Dr. Ali Kalkanlı for permitting the use of facilities of their laboratories.

I would like to thanks the members of the research group in particular Serdar Tan and Rabia Ölmez for their assistance in various aspects of this work.

I am also thankful to the staff of Metallurgical and Materials Engineering department for their help in the various stages of this study.

I am truly indebted to my family Süreyya Kubilay, Ruhi Kubilay and M.Murat Kubilay for their great patience, support and love throughout my education.

TABLE OF CONTENTS

PLAGIARISM.....iii
ABSTRACT..... .iv
ÖZ v
DEDICATION vi
ACKNOWLEDGEMENTS vii
TABLE OF CONTENTS viii

CHAPTER

I.INTRODUCTION 1

II.LITERATURE REVIEW 2
2.1. Introduction 2
2.2. Pore Formation 3
2.2.1 Polymeric Systems 3
2.2.2 Metallic Systems 8
2.3. Foam Stability 13
2.3.1 Aqueous Foams 13
2.3.2 Metal Foams 14

III.EXPERIMENTAL PROCEDURE 20
3.1. Materials 20
3.2. Separation of TiH_2 Powders 21
3.3. Mixing and Compaction of Powders 22
3.4. Foaming 22

IV.RESULTS AND DISCUSSION.....26
4.1. Characterization of Hot Pressed Compacts 26
4.2. Experimental Program.....26
4.3. Foaming of Aluminium.....29
4.3.1. Macroscopic Observation 29
4.3.2. Duration of Foaming 32
4.3.3 Microstructural Observations 34
4.3.4. Effect of TiH_2 Size on Foaming of Aluminium 37
4.3.4.1. Minimum Critical Particle Size 38

V.CONCLUSION 44

REFERENCES 46

CHAPTER I

INTRODUCTION

Metal foams with their low densities and superior mechanical properties are important class of materials. They have a wide potential of applications, such as lightweight structural components, core materials for sandwich structures, heat insulation, radiant shielding, sound, and energy absorption applications.

Depending on the required properties of the foam, different materials are used. Low density materials especially aluminium and aluminium alloys are the most common ones.

To produce aluminium foams, liquid and powder based techniques are used. However, some foaming inhomogeneties can occur during production and they can affect properties of foams adversely. The shape, size and distribution of pores in the matrix should be controlled. Small pores with uniform distibution are the required condition.

In the present work, aluminium foam is produced by powder metallurgy technique and the effect of particle size of foaming agent (TiH_2) on the process of foaming is investigated. Two different sizes of foaming agent are studied; coarse (8,5 μm) and fine (27,5 μm).

CHAPTER II

LITERATURE REVIEW

2.1. INTRODUCTION

In recent years, there has been a growing demand for the use of metallic foams, particularly aluminium foams, for automotive, railway and aerospace applications where weight reduction and improvement in safety is needed (Gibson et al., 1997, Davies et al., 1983). Low density, high energy absorption, heat insulation and other properties make the metallic foams an important class of materials (Körner and Singer, 2000, Banhart, 2000). Aluminium foams can be used in automotive applications especially in the crushable parts to absorb impact energy (Fuganti and Lorenzi, 2000).

Studies concerning metal foams continue for two decades. Metal foams are predominantly closed cells which makes them useful for structural, load-bearing applications, whereas functional applications (filtration, damping etc.) require open cell structures (Banhart, 1999).

Foams may be fabricated with a variety of liquid methods or through powder processing. PM method relies on the mixing of a metal powder with a foaming agent. The foaming agent releases a gas during melting which causes the formation of pores in the liquid metal

Foaming agent used in aluminium and aluminium alloys, is usually TiH_2. However addition of TiH_2 is not enough and an increase in the viscosity of the liquid metal is normally necessary. The viscosity can be adjusted in alloys by a suitable selection of

foaming temperature in between the solidus and liquidus lines or controlled addition of solid particles to the liquid metal.

There are many studies concerning the production methods and properties of foams (e.g. Banhart, 1999, Gibson and Ashby, 1997), however, the physical principles underlying the foaming process are not yet fully understood. Some aspects of metallic foams such as pore nucleation and the stabilization of pore structure are still not fully explored.

2.2. PORE FORMATION

Foam formation studies concentrate on metallic systems as well as on polymeric systems

2.2.1. Polymeric Systems

Colton and Nuh (1987) studied the nucleation of microcellular foam. Microcellular foam is produced by first uniformly stirring a polymer with a gas like nitrogen. Then the temperature is increased and pressure is decreased. Thermodynamic instabilities in the system cause the bubbles to nucleate. This production route is similar in metal foams production via liquid based methods.

Bubble nucleation in polymer foams may occur either homogeneously or heterogeneously. According to Colton and Nuh, for nucleation to occur dissolved gas should have a concentration above the solubility limit. When the concentration is increased, more bubbles nucleate. This is homogeneous nucleation. In heterogeneous nucleation, bubble formation takes place at an interface or at a second phase particle initially present. This occurs when the solubility limit of the additives is exceeded. Above solubility limit, both homogeneous and heterogeneous nucleation takes place.

Fig. 2.1. shows the gas concentration vs. time graph to see the effect of saturation concentration (Klempner and Frisch, 1991). In the first part, the concentration of gas

in solution is lower than saturation concentration therefore, bubble formation cannot be observed. In region II, gas concentration is increased by increasing the temperature and decreasing the pressure. Therefore, in the second region, gas concentration exceeds the critical value and homogeneous nucleation starts. In third region, since the bubbles formed reduce the gas concentration, bubble formation stops. In this region, bubbles grow by diffusion.

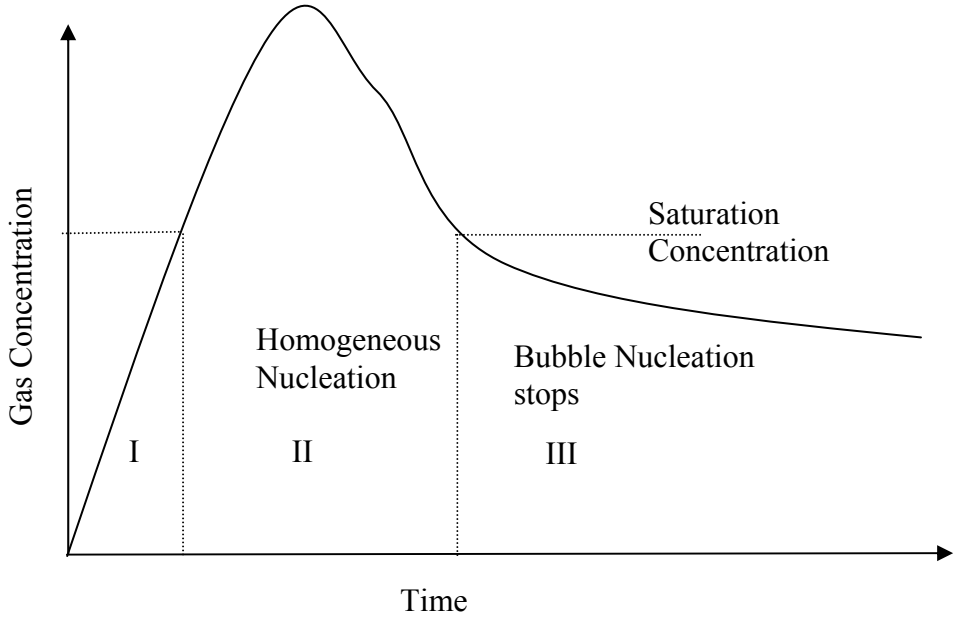

Figure. 2.1. Variation of gas concentration with time. Gas concentration effects the bubble nucleation and growth. (Klempner and Frisch, 1991)

According to Lillico et al. (2001). the energy of the pore, ΔU is defined as:

$$\Delta U = -\frac{4}{3}\pi r^3 f\Delta P + 4\pi r^2 \gamma \qquad \textbf{(2.1)}$$

Here r is the size of the bubble, $f\Delta P$ bubble creation potential per unit volume and γ is the surface energy.

According to Lilico et al. only particles that have larger size than the critical value can form and grow. Capillary pressure inside the small bubbles will cause them to collapse. The critical value can be determined when ΔU reaches maximum as shown in Fig. 2.2.

Shafi et al. (1997) studied on bubble nucleation and growth mechanisms in polymer foams. They used the free energy of critical cluster formation to determine the critical nucleus size. They combine the nucleation rate with bubble growth dynamics. They suggested that once a bubble nucleates, it grows immediately until surface forces are high enough to overcome the viscous forces.

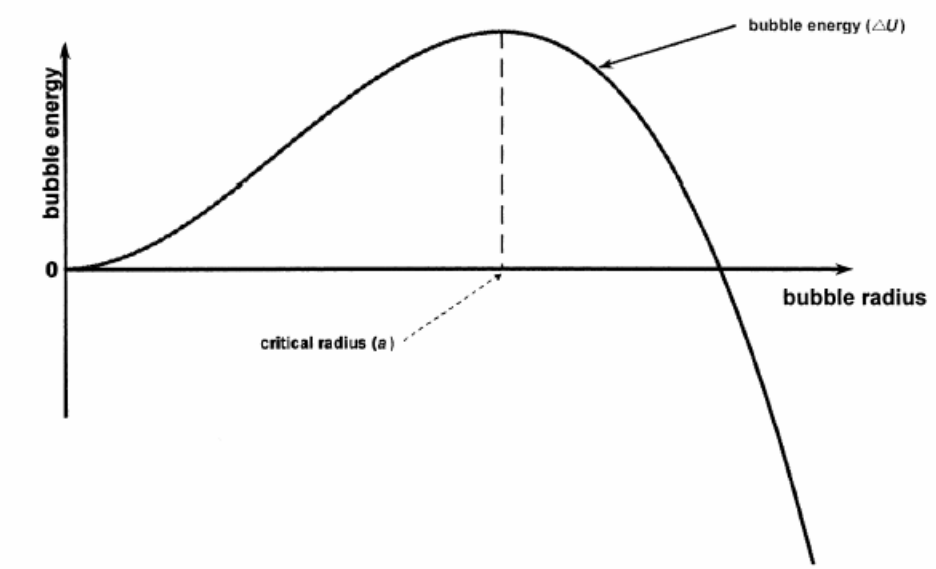

Figure 2.2. Variation of the energy of the bubble with bubble radius. (Lillico et al., 2001).

According to Shafi et al. due to the excess internal pressure inside the bubble, bubble growth occurs. This is except for when bubbles are stabilized by very fine foaming agent/particles where the growth is restricted by the surface energy and viscoelastic effects. Normally growth occurs via diffusion of gas from small bubbles to larger ones according to the pressure difference between them.

$$\delta P = 2\gamma(\frac{1}{r} - \frac{1}{R}) \quad \textbf{(2.2)}$$

Here δ P is the pressure difference between the bubbles, γ is the surface tension, R and r are the radii of the large and small bubbles respectively. As a result of pressure difference between the bubbles, Oswald ripening effect is observed, that is small pores gets smaller and large pores gets larger.

Hobbs (1976) investigated the foaming of thermoplastics using the traditional injection molding equipment. He dissolved the gas in the molten polymer and allowed it to expand as the polymer passed into the mold cavity. According to Hobbs, there is a critical radius of bubbles above which bubble growth takes place. This is due to the reason that pressure inside the small bubbles are higher than the pressure inside the large bubbles and therefore diffusion direction is from small bubbles to larger ones. As external pressure is decreased, critical radius above which bubble nucleation starts falls down.

According to Chernyak (1959) for bubble to grow the following condition must be satisfied;

$$P_g - P_l = \frac{2\gamma}{r} \quad \textbf{(2.3)}$$

Here P_g is the gas pressure inside the bubble, P_l is the pressure of the liquid surrounding the liquid, γ is the surface tension and r is the radius of the bubble.

Arefmanesh and Advani (1990) produced the polymer foams by dispersing a chemical blowing agent in the polymer by pre-blending. The mixture is then melted under pressure. Meanwhile, the blowing agent is decomposed at a high temperature to release a certain type of gas, but at this stage, all the gas remained dissolved in the melt due to the applied pressure. Then the mixture is injected into the mold cavity

maintained at low pressure. At this point, the melt becomes supersaturated and bubbles nucleate and grow to fill the mold cavity.

Arefmanesh and Advani used a cell model to explain the bubble growth. The growth in a Newtonian fluid under isothermal condition as in the above study follows,

$$R = \frac{1}{4\mu}(P_g - P_f)R - 2\gamma \tag{2.4}$$

Here R is the rate of bubble growth (in terms of radius), μ is the viscosity, γ is the surface tension, P_g is the gas pressure inside the bubble, P_f is the fluid pressure at the outer boundary of the cell, Fig. 2.3.

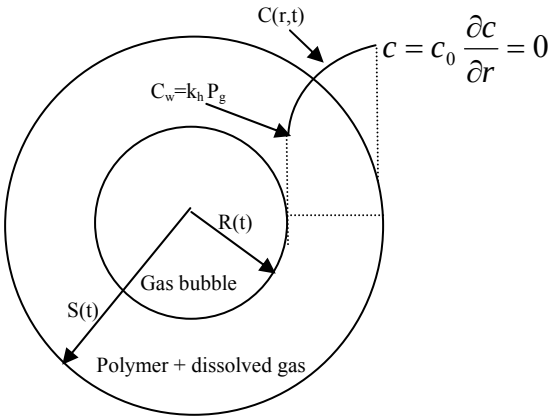

Figure 2.3. Bubble Growth Model according to Arefmanesh and Advani 1990. R(t) is the time dependent bubble radius, S(t) is the outer diameter of the cell depending on time and C is the gas concentration.

In this model, concentration of the dissolved gas at the bubble interface is related to the gas pressure inside the bubble with Henry's law.

$$C_w = k_h P_g \tag{2.5}$$

where C_w is the concentration of the dissolved gas at the interface and k_h is the Henry's constant. Initially gas concentration is equal to C_0 and changes with time due to diffusion of gas from liquid to the bubble.

Amon and Denson (1984) also used the cell model to study the dynamics of foam growth and developed a model for the growth of spherical bubble surrounded by a thin sheet of liquid. The cell model is developped by assigning a specific amount of liquid to each individual bubble in a liquid pool that contains a large number of bubbles. The unit cell is taken to be spherical and consists of a single gas bubble and a concentric liquid envelope or shell.

2.2.2 Metallic systems

Metallic foams can be produced in a manner similar to polymeric foams, i.e. by injecting gas into the liquid metal and expanding it inside a mold (e.g.). However most studies make use of solid foaming agent which generates gas when the preform is heated up to elevated temperature.

Foaming agent for aluminum and aluminum alloys are usually TiH_2. TiH_2 when heated to 550°C decomposes (Kennedy, 2003).

$$Ti_{H2} = Ti + H_2$$

Thus the foaming agent decomposes and generates hydrogen which expands the liquid metal.

In models considering the bubble formation, gas inside the bubble is accepted as ideal (Fusheng et al., 2003). Therefore the pressure inside the bubble

$$P_{in}\, V = n_{H2}\, R\, T \qquad \textbf{(2.6)}$$

Here P_{in} is the pressure inside the bubbles, V is the volume of the bubble, n_{H2} is the number of moles of hydrogen in the bubble, R is the universal gas constant, T is the temperature (K). Since bubble is spherical

$$V = \frac{4}{3}\pi r^3 \tag{2.7}$$

Eq. 2.6 can be written as,

$$P_{in} = \frac{3n_2 RT}{4\pi r^3} \tag{2.8}$$

As seen, the pressure inside the bubble depends on the amount of gas released.

According to Degischer and Kristz (2002) bubble growth follows Rayleigh equation:

$$R\dot{R} + \frac{3}{2}\dot{R}^2 + \frac{4\nu\dot{R}}{R} = \frac{1}{\rho}(P_{in} - \frac{2\gamma}{r} - P_{eq}) \tag{2.9}$$

Here P_{in} is the pressure inside the bubble, P_{eq} is the equilibrium pressure in the liquid, γ is the surface tension, ν is the kinematic viscosity, ρ is the density and r is the radius of the bubble. In equation 2.9, the left hand side of the equation is the inertia and viscous forces. They are against the bubble growth. If these forces are neglected, Rayleigh equation takes the form of:

$$P_{in} = P_{eq} + 2\frac{\gamma}{r} = P_0 + \rho g h + 2\frac{\gamma}{r} \tag{2.10}$$

Here g is the gravitational constant, h is the depth of the bubble from the bottom and P_0 is the ambient pressure. This equation shows the equilibrium condition for bubble formation at gas-liquid interface. Ambient pressure in Rayleigh equation is taken as atmospheric pressure and hydrostatic pressure is given as;

$$P_h = \rho g h \tag{2.11}$$

Here P_h is the hydrostatic pressure, ρ is the density of the metal, g is the gravitational acceleration, h is the height of the liquid metal over the bubble.

Edwards and Pithia (1995) proposed that critical nucleus size can be determined by external pressure and temperature and Rayleigh equation controls the expansion of the nucleation site. The definition of the critical particle size is given as the value of the radius, at which the breakdown of liquid will occur,

$$r = \frac{2\gamma}{\Delta p} \qquad \textbf{(2.12)}$$

Here γ is the surface tension and Δp is the pressure difference between the nuclei and imposed pressure.

In pore formation, pressure generated inside the bubble is related to decomposition of foaming agent Tan (2003). In the case when foaming agent is TiH_2,

$$Ti_{H2} = Ti + H_2 \qquad \textbf{(2.13)}$$

The reaction is reversible and occurs according to well known van't Hoff equation. According to Mueller et al. (1968) the van't Hoff equation for TiH_2 has the form:

$$\ln P_{eq} = \frac{-19821}{T} + 21.671 \qquad \textbf{(2.14)}$$

Fusheng et al. (2003) indicated the necessary condition for bubble formation. Gas pressure inside the pore, $P_{in,}$ should be high enough to overcome the external pressure. External pressure consists of hydrostatic pressure, $P_{h,}$ of the melt, atmospheric pressure, $P_{a,}$ and pressure due to surface tension, P_s.

$$P_{in} > P_{ext} = P_h + P_a + P_s \qquad \textbf{(2.15)}$$

As in the case of polymer foams, there is a critical foaming agent size to start foaming in metallic system. Necessary condition for bubble nucleation is explained by Tan (2003), that is equilibrium pressure should be high enough to overcome the pressure over TiH_2. Therefore the required condition for foaming:

$P_{eq} >= P_{ext}$ **(2.16)**

In order to satisfy this condition, TiH_2 particle should decompose which will occur below and up to a certain level of pressure at a given temperature. For bubble to grow this pressure should be equal or greater than P_{ext}. Therefore, there is a critical particle TiH_2 size necessary for foaming. At constant temperature, only particles that are larger than the critical particle size can release their hydrogen for bubble formation.

The minimum critical particle size given in Fig. 2.4., is determined by the intersection point of P_{ext} and P_{eq} Tan (2003).

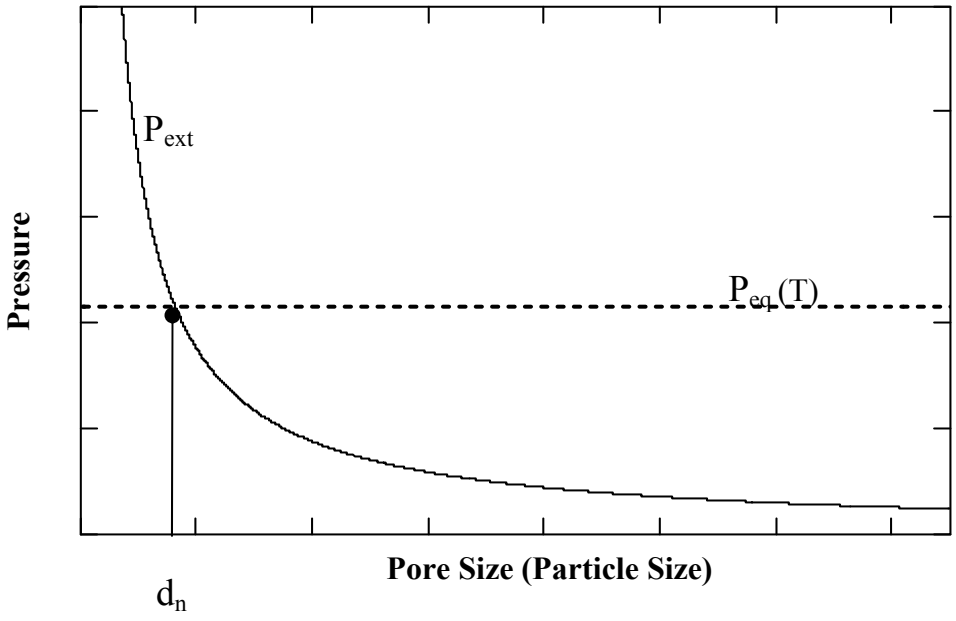

Figure 2.4. Schematic variation of P_{eq} and P_{ext} with pore size at constant temperature. Note that their intersection point gives the critical size of foaming agent (Tan, 2003)

In the model presented by Tan (2003), hydrostatic pressure and atmospheric pressure are ignored in P_{ext} equation and therefore P_{ext} is equals to:

$$P_{ext} = P_s = \frac{2\gamma}{r} \quad \textbf{(2.17)}$$

As long as pressure inside the bubble is larger than external pressure, hydrogen generation continues.

$$P_{in} > P_{ext} \quad \textbf{(2.18)}$$

Therefore, when P_{in} equals to P_{ext}, a new parameter is introduced by Tan (2003). This is the equilibrium pore size and shows the maximum pore size that can be achieved by constant hydrogen release. Equilibrium pore size can be determined by the intersection point of P_{ext} and P_{in} when all the hydrogen is released.

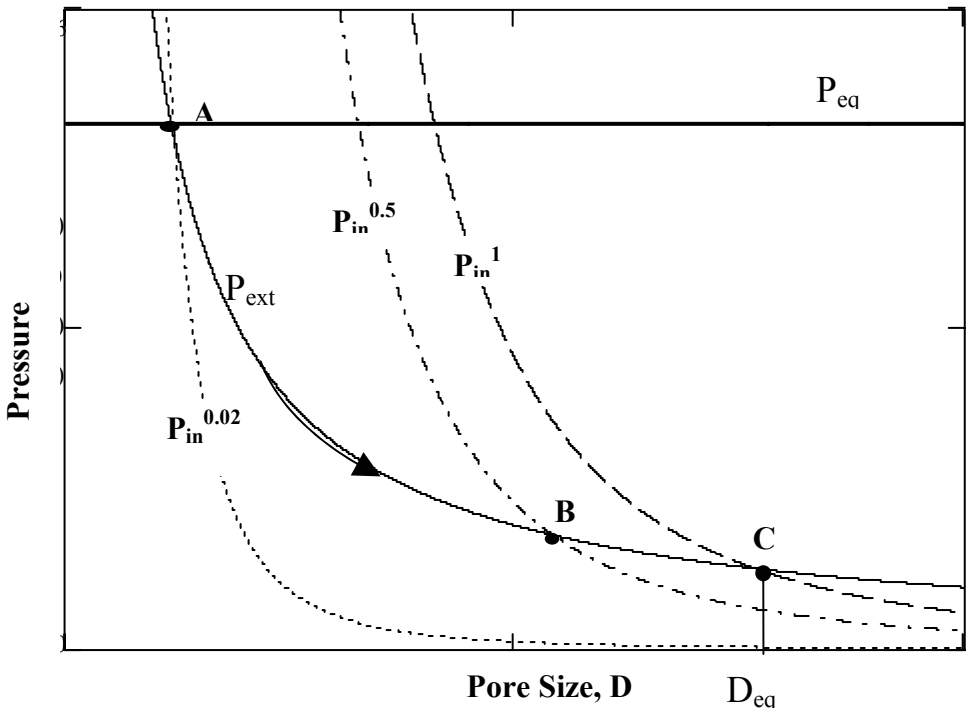

Figure 2.5. Schematical drawing of variation of P_{in} and P_{ext} with pore size. Superscript in P_{in} shows the fraction of hydrogen released by TiH_2. Note that D_{eq} is defined as the intersection of P_{ext} with P_{in}^{1}, Tan (2003).

2.3. FOAM STABILIZATION

Foams are out of equilibrium systems therefore for successful foam production, it is important to stabilize the bubbles. Viscosity of the system is the main factor determining the stability. Viscosity of the system can be adjusted by the solid fraction in the melt, i.e. in alloys by controlling the melt temperature between the solidus and liquidus or via addition of solid particles (carbide, oxide and other ceramic particles) to the melt.

There are many studies on the foam stabilization especially on aqueous foam (e.g. Tang, 1989, Garret, 1979, Wübben, 2002)

2.3.1 Aqueous Foams

Tang et al (1989) investigated the effect of adding SiO_2 particles on foam stabilization. In this study, foam is produced by sodium dedocyl sulfonate in alkaline aqueous medium. According to them, the most important factor that should be considered in foam stabilization is the particle size of the added material i.e.SiO_2. As the particle size decreases, foam stability increases.

Hudales and Stein (1990) studied the influence of the hydrophilic glass particles in cetylmethylammonium bonde (CTAB) solution. The particles used were between 1 and 10 μm. In addition, they concluded that large particles are effective to delay foam drainage and increase foam stability. They also indicated that hydrophilic particles smaller than 1 μm shorten the lifetime of foams.

While considering the aqueous foams, in some cases it is necessary to reduce the foamability of the solution. Antifoams, which are usually insoluble additives, are used for this purpose. They either prevent foam formation or break down foam which has already been formed. Garrett (1979) studied the behaviour of foam in the presence of polytetrafluorethylene (PTFE) particles. He suggested that hydrophobic materials are effective in antifoam mechanism. The effectiveness of PTFE particles

is associated with particle size and shape. Frye (1989) also used hydrophobic solid particles like teflon to destabilize the foam.

2.3.2 Metalic Foams

Foam stability in metallic systems is also studied. In metals, viscosity is the main factor effecting the stabilization. Viscosity should be adjusted in an optimum value for successful foaming.

According to Wübben et al (2002), finely dispersed ceramic particles may stabilize the foam in three different ways; they could increase the viscosity of the melt (this will prevent the flow of metal out of the foam film.), they could decrease the surface tension of the metal, and they could delay or prevent rupture of films separating the bubbles. They indicated that for foam stabilization, adding non-metallic particles is important. However, if powder metallurgy route is used for foam production, no additive is needed since oxide film on the surface of the particles may act as additives.

Particle size and volume concentration of the stabilizing particles are very important in considering the viscosity. According to Kaptay (2003) there is an optimum viscosity for foaming, Fig. 2.6.

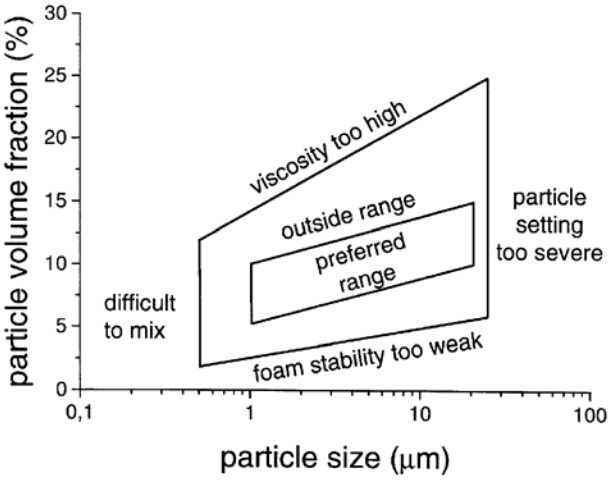

Figure 2.6. Foaming map in terms of size and volume fraction of stabilizing agent. Note that there is an optimum range for foaming. (Kaptay, 2003)

According to Kaptay, too fine ceramic particles cannot be mixed with liquid metal easily forming "difficult to mix" region in Fig. 2.6. This is due to their high surface tension. In the "viscosity too high" region, foaming does not take place as too high viscosity suppresses the bubble formation and growth. In "particle settling too severe" region, particles tend to settle to the bottom of the vessel, this means that added particles are not capable of attaching themselves the bubbles to attain the stability. When viscosity is too low, i.e. "foam stability too weak" region in Fig. 2.6, foam collapses before it solidifies. The reason of this is the drainage, i.e. the slow flow of liquid out of the cell walls, due to gravity. If the volume concentration of the ceramic particles is too low, they are not enough to stabilize the foam and therefore foam stability is weak.

According to Song et al. (2000), if viscosity is too low, it will cause bubbles to float rapidly and too high viscosity will prevent the bubble formation. Song et al. also indicated that adding Ca into the melt is effective in increasing viscosity. Addition of calcium makes the oxidation stronger and as the amount of oxide increases, apparent viscosity increases. However, the increase in viscosity declines becomes less with the increase of Ca. Calcium also increases the pore number and decreases the pore size. Miyoshi et al. (2000) also used calcium to increase the viscosity by increasing the oxidation susceptibility of the foam.

Ceramic particles such as SiC, Al_2O_3 are most commonly used for melt stabilization (Deqing and Ziyuan, 2003, Leitlmeier et al., 2002, Yang and Nakae, 2000). According to Bretsznajder (1971) the viscosity of liquids containing solid particles is given by,

$$\eta = \eta_0 \left[1 + \frac{2X}{\left(1 - 1.2X^{2/3}\right)^2} \right] \qquad \textbf{(2.19)}$$

Here η is the viscosity of the liquid, η_0 is the virgin liquid' viscosity, X is the particle concentration.

Another important parameter in stabilization of foams is the surface tension. Surface tension is the energy required to increase the surface area of a material by a unit amount. The effect of various alloying elements on the surface tension of Al is given in Fig. 2.7. Park (2002) defined the optimum condition for metal foaming as low surface tension and high viscosity. Viscosity affects the pore size of the foam also. With increasing viscosity, size of the bubbles decreases but # of pores per unit volume increases. (Song et al., 2000 and Yang and Nakae, 2000).

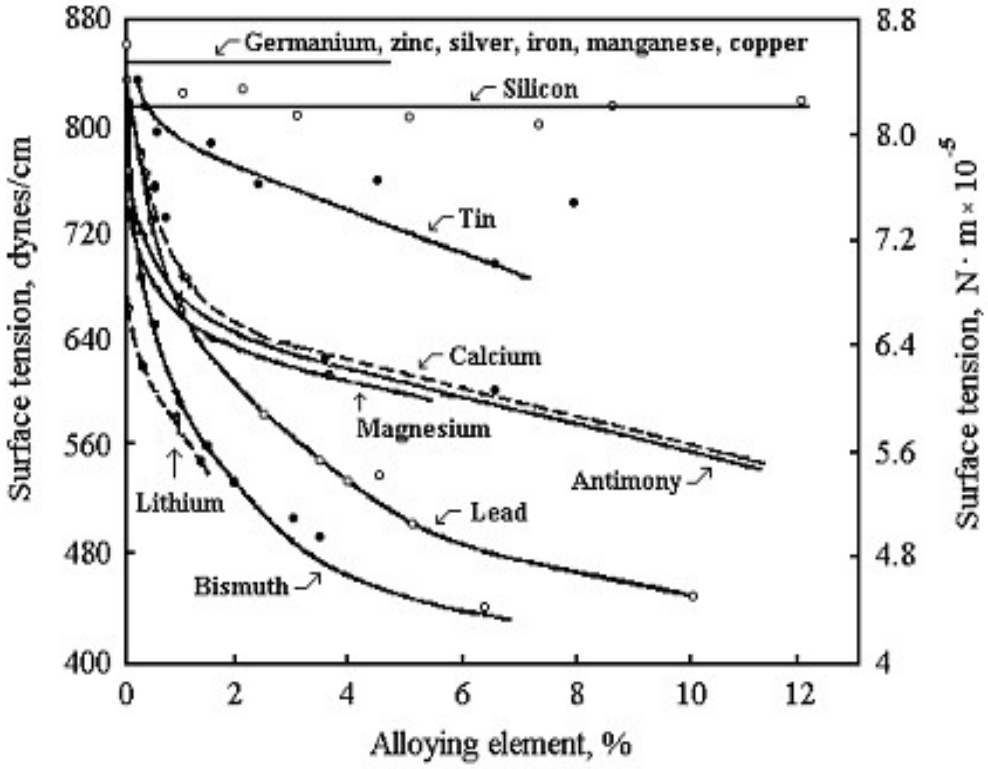

Figure 2.7. Effect of alloying elements on the surface tension of Al (Horn, 1967).

According to Yang and Nakae (2000), another role of the ceramic particles is that they serve as nucleating agents for bubbles to form and grow. Deqing and Ziyuan (2003) investigated the stabilizing effect of the particles as a function of their particle size and volume concentration. According to their results, cell size and wall thickness is highly dependent on addition of SiC or Al_2O_3 particles. Particles are effective in increasing cell size and wall thickness at constant temperature. The

increase in cell wall thickness means that cell wall drainage is retarded. Therefore, more stable foam is achieved. There is a critical particle concentration at which stable foam formation takes place. If particles are added excessively, unstable foam formation takes place. They concluded that for stable Al foam, using 3.5 μm particles the volume fraction should be below 14 % whereas for 10 μm particles, the volume fraction should be 15 % or higher . If the added particles are 5 μm, the required concentration is 14-17.5 %. They also indicated that increasing the foaming temperature decreases the cell wall thickness. This is due to the reason that at higher temperatures, the viscosity is lower.

As explained, stability of the foam is greatly dependent on viscosity. Another parameter that influences the viscosity of the liquid is the temperature. This dependency is studied by Battezati and Greer (1989), Andrade (1934), and Hirai (1993). According to them, temperature dependency of viscosity can be described simply by an Arhennius equation:

$$\eta = n_c \cdot e^{\left[\frac{\left[2.65\left(T_m\right)^{1.27}\right]}{8.314\cdot(T)}\right]} \qquad \textbf{(2.20)}$$

$$\eta_c = \frac{\left[1.7\cdot 10^{-7}\cdot(d\cdot 1000)^{\frac{2}{3}}\cdot\sqrt{T_m}\cdot\left(Mw\cdot 10^{-3}\right)^{\frac{-1}{6}}\right]}{e^{\left[\frac{\left[2.65\left(T_m\right)^{1.27}\right]}{8.314\cdot\left(T_m\right)}\right]}} \qquad \textbf{(2.21)}$$

Here, d is density of metal (gm/cm^3), T_m is melting temperature of the metal (K), Mw is molecular weight of the metal (g/mol), η_c is viscosity coefficient (Pa·s) and η is viscosity of the metal at temperature T (Pa·s). This equation as applied for aluminium is plotted in Fig 2.8., which shows the temperature dependency of the viscosity

Foam stability is greatly dependent on the drainage of the cell wall separating the bubbles. Drainage is the steady removal of the liquid from the foam. In drainage

gravity force, capillary (surface tension) and viscous forces are effective (Koehler et al., 1998, Stone et al., 2003, Gergely and Clyne, 2004). Generally, gravity and capillary forces are in favor of drainage and viscous forces are against drainage. Gergely and Clyne studied on the drainage in liquid foams. They concluded that, as drainage occurs a vertical gradient develops in the capillarity pressure. This term is partially effective in preventing drainage. Fine pore sizes and high porosity are effective in decreasing drainage probability since they increase the capillarity pressure.

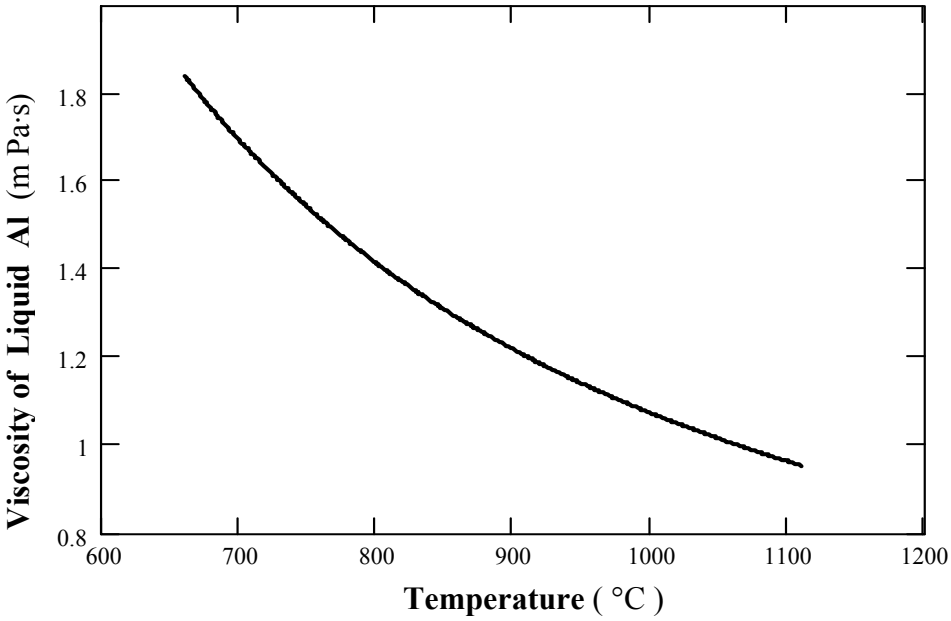

Figure 2.8. Temperature dependency of the viscosity for liquid Al (Derived from Eq. 2.21)

The ceramic particles added to increase viscosity are also effective in decreasing the drainage probability. Deqing and Ziyuan (2003) increased the cell wall thickness by agglomerating near the liquid-gas interface. This cell wall act as a barrier to liquid flow therefore drainage is retarded.

Drainage concept is investigated in two terms (Koehler et al., 1998). Free drainage and forced drainage. Free drainage is the most important one in formation of foams.

This is mainly the drainage due to gravity and liquid flows until the equilibrium is attained. Foam dries first at the bottom and liquid drains and accumulates at the bottom. Forced drainage is the steady flow through otherwise static foam, which can be produced by continuous addition of liquid at the top (Jalmes and Langevin, 2002).

CHAPTER III

EXPERIMENTAL PROCEDURE

3.1. MATERIALS

Base metal was pure aluminium (Al) with an average particle size of 37 μm. Additives were alumina (Al_2O_3) and TiH_2. Alumina was added to Al with amounts ranging from 0 to 14 vol %. It was in the form of powders 5 μm (average) in size.

Two sizes of TiH_2 powders were used in the experiments. TiH_2 of fine size had a mean size of 8,5 μm. That of coarse size had an average value of 27,5 μm. Particle size distributions of TiH_2 are given in Fig 3.1. The amount of TiH_2, was 0,6 wt % in all samples.

3.2. SEPERATION OF TiH_2 POWDERS

Coarse and fine TiH_2 were obtained from the as- received TiH_2 powders. The powder was -325 mesh, i.e. in the form of particles that are smaller than 44 μm. Coarse powders were separated from the as received powders by sieving with - 400 mesh sieve. The average size of the coarse particles was 27,5 μm, see Fig. 3.1.

Fine powders were separated from the as received powders via a centrifugial technique. For this purpose, the powders, 1.5 gr, were poured to the center of a glass disc and rotated with the speed of 700 rpm approximately for 1 minute. Coarse powders were thrown away from the disc and the fraction that remained on the disc was collected. This procedure was repeated four times.

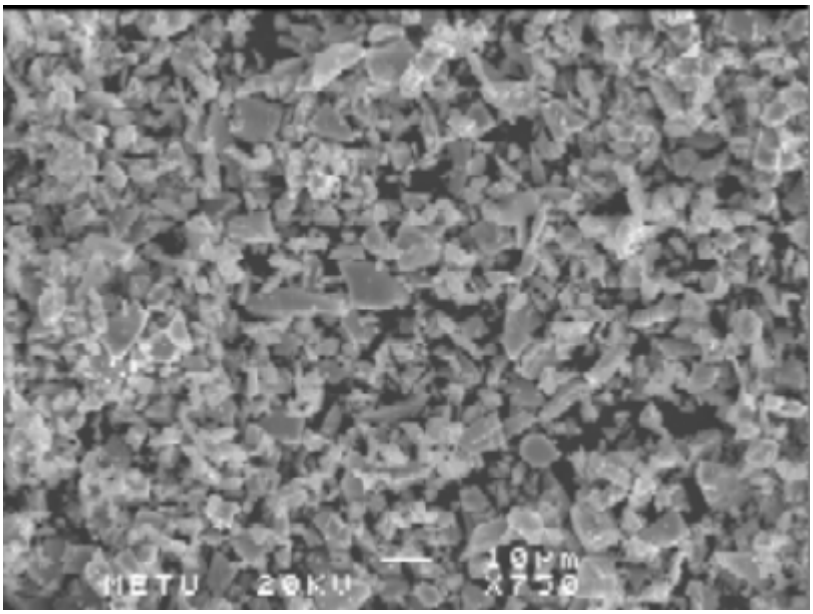

(a)

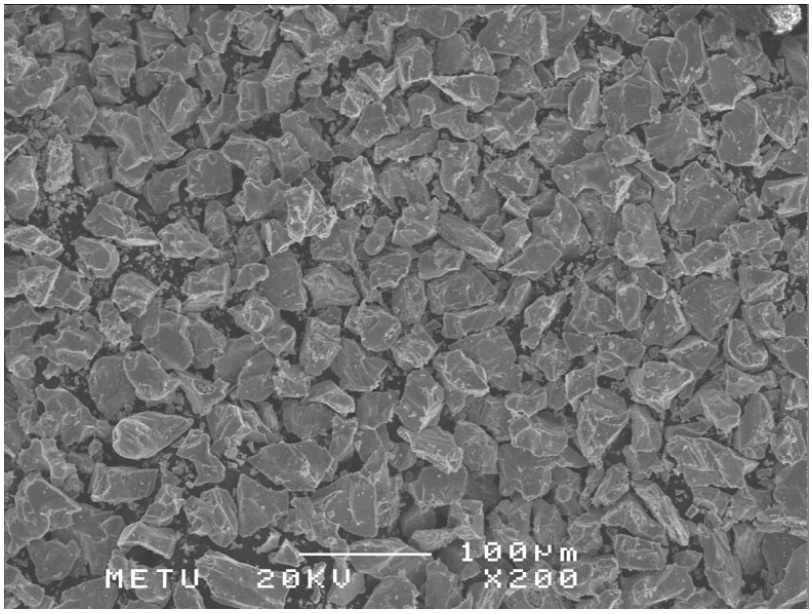

(b)

Figure 3.1. SEM image of TiH_2 particles. a)fine TiH_2 , b)coarse TiH_2.

Fine powders obtained in this manner are shown in Fig. 3.1. It is observed that though some are some coarse particles, the most particles have sizes less than 10 μm.

3.3. MIXING AND COMPACTION OF POWDERS

Powders were mixed with two different methods. For the mixtures with coarse TiH_2 are mixed with a shaker. A plastic bottle of 600cm^3 volume was used as a mixing chamber. 8 grams of powder was mixed for one hour in each batch with ball-to-powder (B/P) ratio of 1:1 using steel balls of 6 mm diameter. The reason for using shaker for coarse powders was to prevent or minimize the powder breakage, which would deacrease the particle size.

Powders containing fine TiH_2 were mixed in a ball mill (40 mm inner diameter) operated at 200 rpm. The ball-to-powder (B/P) ratio is 1:1 using the steel balls of 6 mm in diameter. Again, 8 grams of powder was mixed for one hour in each batch.

The mixed powders were compacted into a cylindrical form by hot pressing method. The pressing was carried out at 400°C for one hour while maintaining a pressure 278 MPa. After hot pressing, samples were in the form of pellets of 15 mm in diameter with a height varying between 8 to 10 mm.

3.4. FOAMING

Foaming experiments are carried out in a tube furnace shown schematically in Fig 3.2. Foaming was achieved in a stainless steel tube inserted into the furnace.

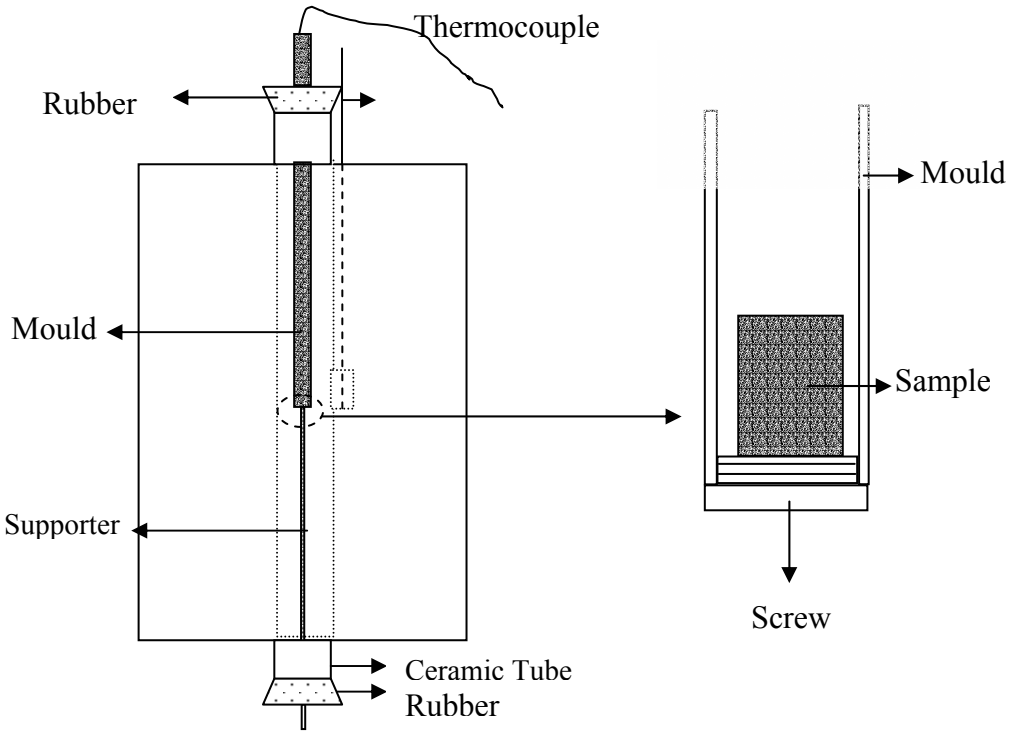

Figure 3.2. Schematic drawing of the set-up used in the foaming experiments.

When the tube reaches the desired temperature, monitored by a thermocouple inserted into the tube, the thermocouple was removed and the pellet is dropped into the tube. Heating rate was therefore very high. From the top, foaming was monitored and when the rising of the liquid metal stopped, experiment was terminated by removing the tube from the furnace. The tube was cooled as soon as it was removed by forced air. The duration of foaming therefore was not constant but varied (1 minute to 30 minutes) from sample to sample.

CHAPTER IV

RESULTS AND DISCUSSION

4.1. CHARACTERIZATION OF HOT PRESSED COMPACTS

Hot pressed compacts were cut in cross section and examined by scanning electron microscope. Fig 4.1 shows a sample (Al-8vol% Al_2O_3-fine TiH_2) with fine TiH_2. In this figure, white particles are Ti i.e TiH_2 particles and black particles are Al_2O_3 particles. As it can be seen the size of the fine TiH_2 particles are quite fine, in fact finer than what was added initially implying that further refinement occurred during milling . In some regions, TiH_2 particles are agglomerated,

Cross-section of a sample (Pure Al, coarse TiH_2) with coarse TiH_2 is given in Fig. 4 2. TiH_2 particles in this sample are very much coarser than those observed above and appear to have a size in the range 20-40 μm .

4.2. EXPERIMENTAL PROGRAM

Effect of the TiH_2 size on foaming was investigated regarding three different parameters: temperature of foaming, solid addition in the melt and the melt viscosity. Experimental program followed is given in Table 4.1. The same program was applied for both systems with fine and coarse TiH_2 seperately.

Experimental program given in Table 4.1 is arranged in the order of increasing viscosity. The expected viscosity of the systems was calculated by considering the temperature and the solid, i.e. Al_2O_3 content of the liquid.

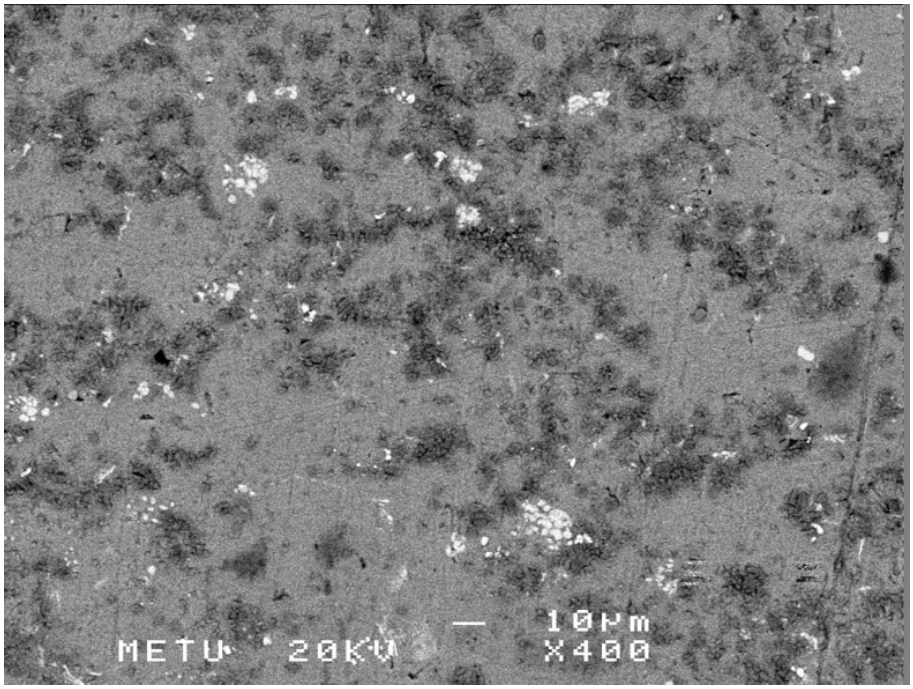

Figure 4.1. SEM image of hot pressed Al pellet with fine TiH_2 (Al-8vol% Al_2O_3-fine TiH_2).

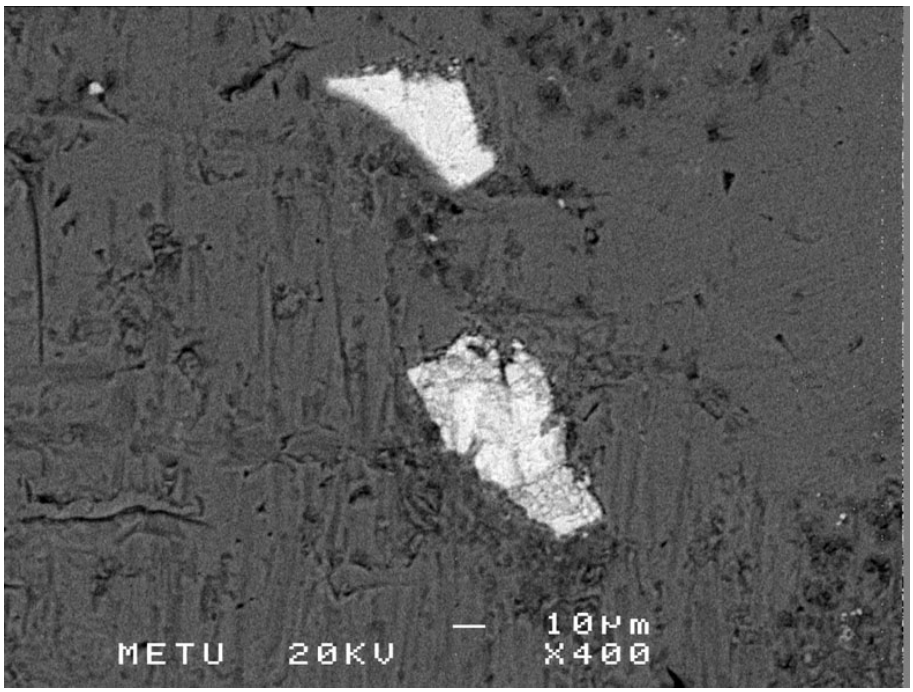

Figure 4.2. SEM image of hot pressed Al pellet with coarse TiH_2 (Pure Al, coarse TiH_2).

Table 4.1. Experimental program

Expected Viscosity (mPa.s)	**Al**	**Al-8 vol % Al_2O_3**	**Al-10 vol % Al_2O_3**	**Al-12 vol % Al_2O_3**	**Al-14 vol % Al_2O_3**
1,70	700°C	835°C			
1,80	675°C	805°C			
2,20		690°C	770°C		
2,32			700°C	740°C	
2,42				690°C	735°C
2,57			680°C	720°C	

For the viscosity of pure aluminium, η_o, a relation given by Battezati (1989) and Hirai (1993) was used i.e.,

$$\eta_o = n_c e^{\left[\frac{\left(2{,}65(T_m)^{1{,}27}\right)}{8{,}314(T)}\right]} \quad \textbf{(4.1)}$$

Here T is the temperature at which the viscosity is calculated and T_m is the melting temperature of the metal both in degrees Kelvin.

The viscosity calculated was corrected for solid content with the use of equation given by Bretsznajder (1989). i.e.,

$$\eta = \eta_o \left[1 + \frac{2X}{\left(1 - 1{,}2X^{2/3}\right)^2} \right] \quad \textbf{(4.2)}$$

Here η is the viscosity of the liquid containing solid particles, η_o viscosity of the liquid without particles and X is the volume fraction of the solid particles.

Figure 4.3 shows the variation of viscosity as a function of both temperature and the solid content.

4.3. FOAMING OF ALUMINIUM

4.3.1 Macroscopic observations

A typical example of foaming is given in in Fig 4.4, which refers to sample with 8% Al_2O_3, coarse TiH_2 foamed at 805°C. In order to see the foam structures the samples cylindirical in shape were cut longitudinally. Fig. 4. 4- 5 show such longitudinal sections of the samples with fine and coarse TiH_2 respectively.

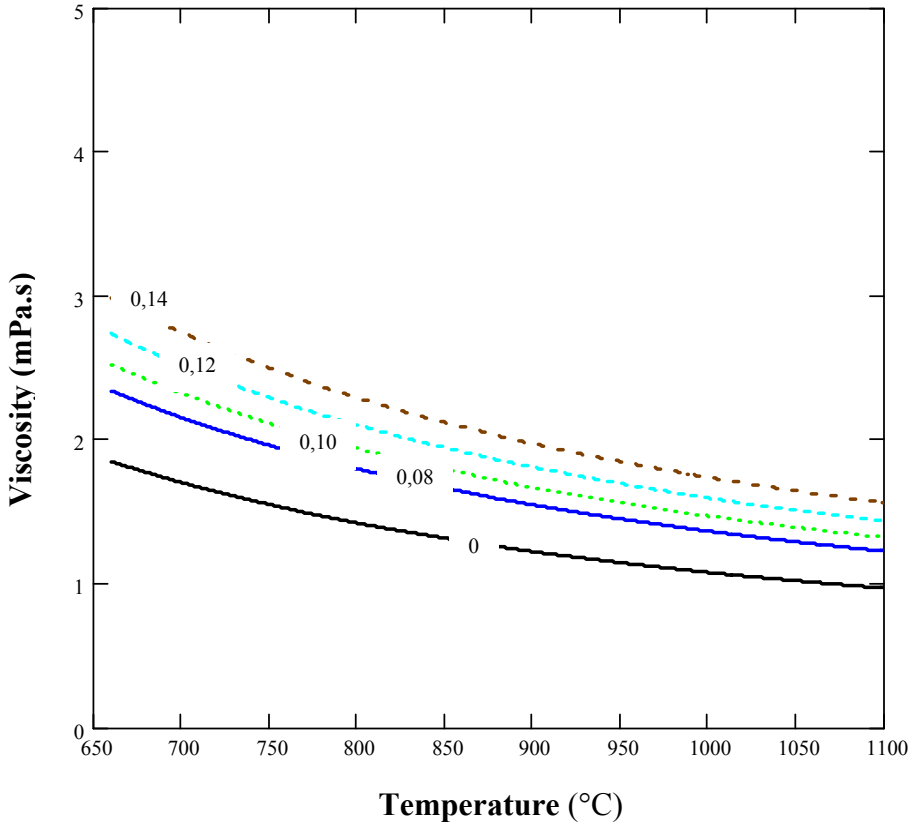

Figure 4.3. Temperature dependence of Al viscosity at various level of solid addition.

Figure 4.4. Photograph of a sample before and after foaming. (Al-8% Al_2O_3-coarse TiH_2) The samples are 15 mm in diameter.

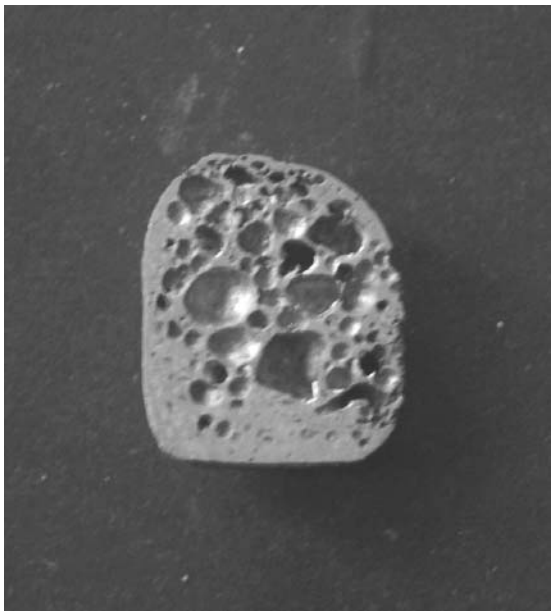

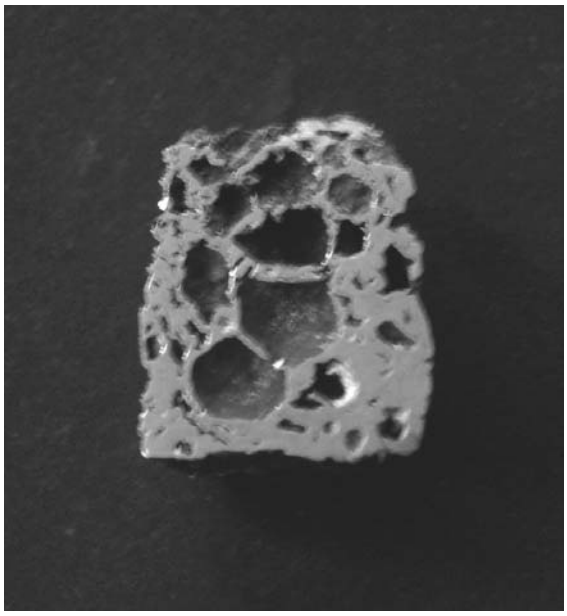

(a) Al + fine TiH_2 , 700 °C **(b)** Al + 8 vol % Al_2O_3 + fine TiH_2 , 805°C

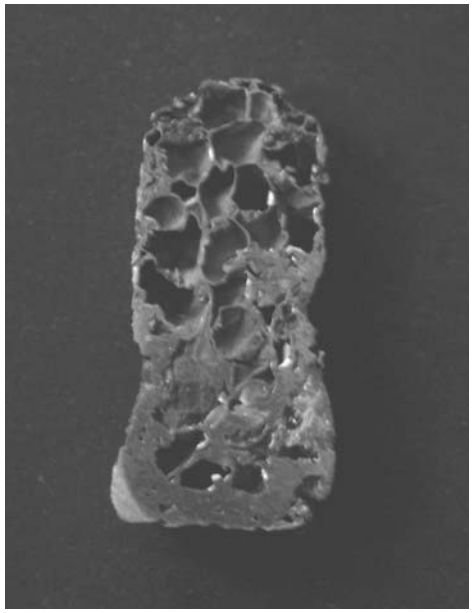

(c) Al + 8 vol % Al_2O_3 + fine TiH_2 ,835°C

Figure 4.5. Longitudinal section of the foamed samples with fine TiH_2. (Diameter: 15 mm)

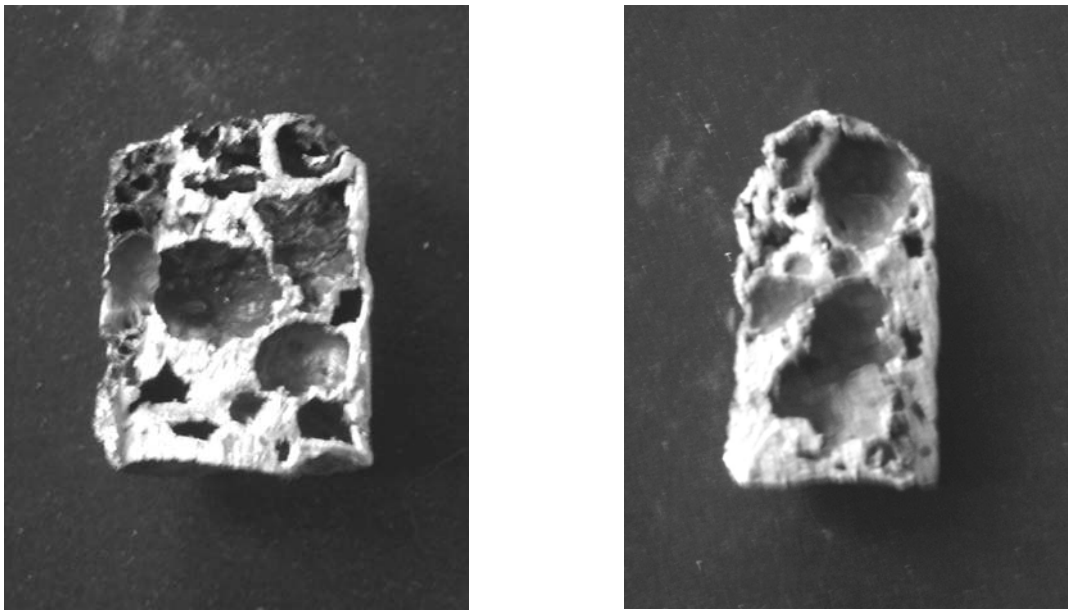

(a) Al + coarse TiH_2 , 700°C **(b)** Al + 8 vol % Al_2O_3 + coarse TiH_2 , 805°C

Figure 4.6. Longitudinal section of the foamed samples with coarse TiH_2. (Diameter: 15 mm)

Fig. 4. 4- 5 show such cross sections. Fig. 4.5 refers to samples with fine TiH_2. It is seen that the sample foamed at 700°C; the pores are small and almost evenly distributed. The correrssponding structure with coarse TiH_2 is given in Fig. 4.6 (a). It may be stated that the pores with fine TiH_2 appears to be smaller than those obtained with coarse TiH_2, compare Fig. 4.5 (a) and 4.6 (a). At higher foaming temperatures both samples yield pore sizes in the order of 3-4 mm.

4.3.2 Duration of foaming

Fig. 4.7 shows the duration of foaming with respect to foaming temperature for both systems; fine and coarse TiH_2. It seen that time required for foaming decreases with increasing foaming temperature, especially at temperatures above 800°C, a few minutes is enough to achieve desirable degree of foaming whereas at lower temperatures the time can be as long as 30 minutes. The size of the foaming agent influences the time required for foaming. In fine systems, the time required appears to be less than the coarse systems. If the duration of foaming increases too much, foam structure may collapse as in Fig. 4.8.

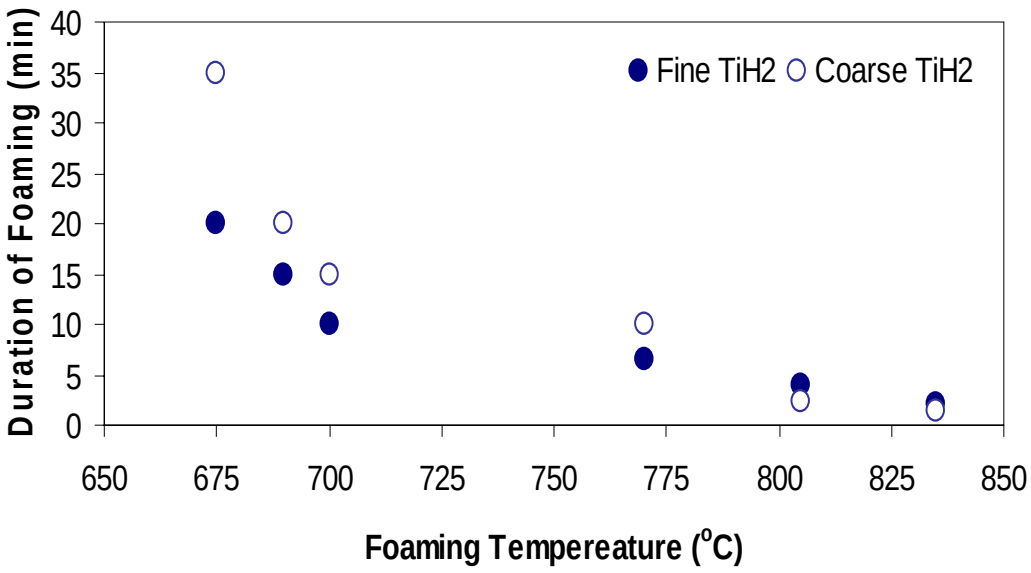

Figure 4.7. Duration of foaming with respect to temperature.

Figure 4.8. Photograph of a collapsed foam. (Al-8% Al_2O_3-fineTiH_2, 805°C) (Diameter: 15 mm)

4.3.2 Microstructural observations

The cross sections of the samples are also investigated in scanning electron microscope. An image of the pores in a sample containing pure Al and fine TiH_2 foamed at 675°C is seen in Fig. 4.9.

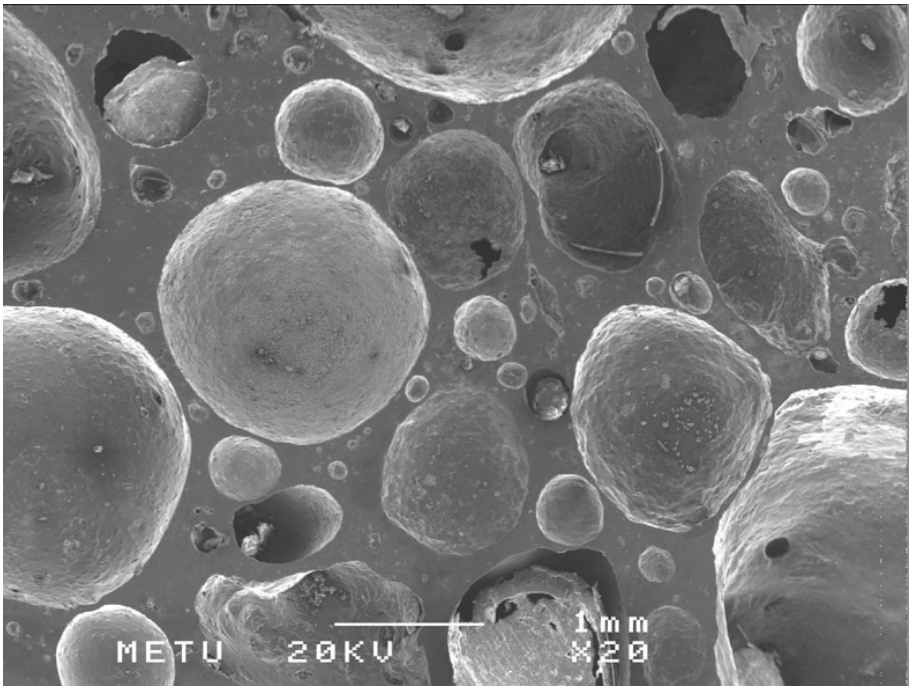

Figure 4.9. An image of the pores in Al foam. (fine TiH_2, 675°C)

Fig 4.10 shows more details in the pore walls. EDAX analysis taken from the pore wall is given in Fig 4.11. Relatively high concentration of oxygen in the EDAX in these regions was interpreted as the the prefential accumulation of Al_2O_3 particles in the pore walls. Another example of pore structure is given in Fig. 4.12.

Foaming agent, i.e. TiH_2 can also be observed in foamed samples, Fig. 4.13. shows an example. Here the particles that are embedded have two regions; an outer grayish region and white inner core. The EDAX analysis taken from the core yields titanium (or perhaps TiH_2 since hydrogen cannot be detected with the EDAX used). The surrounding grayish layer contains both titanium and aluminium in amounts that comply with intermetallic Al_2Ti.

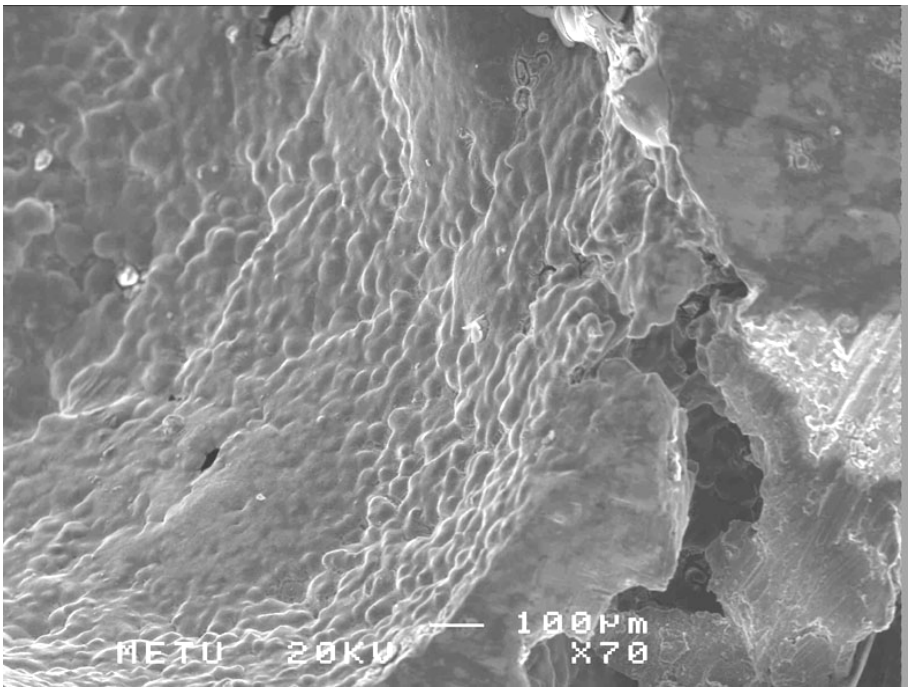

Figure 4.10. Typical pore walls in a foamed sample. (Al-8% Al_2O_3-fineTiH_2, 805°C)

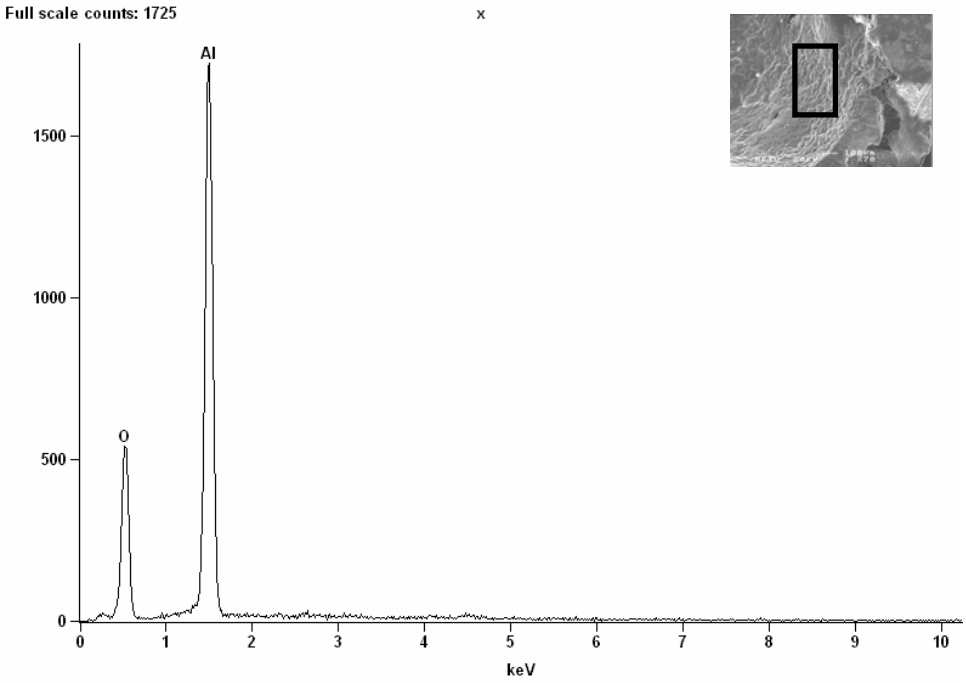

Figure 4.11. EDAX analysis taken from the pore walls in Fig. 4.10. (Al-8% Al_2O_3-fineTiH_2, 805°C).

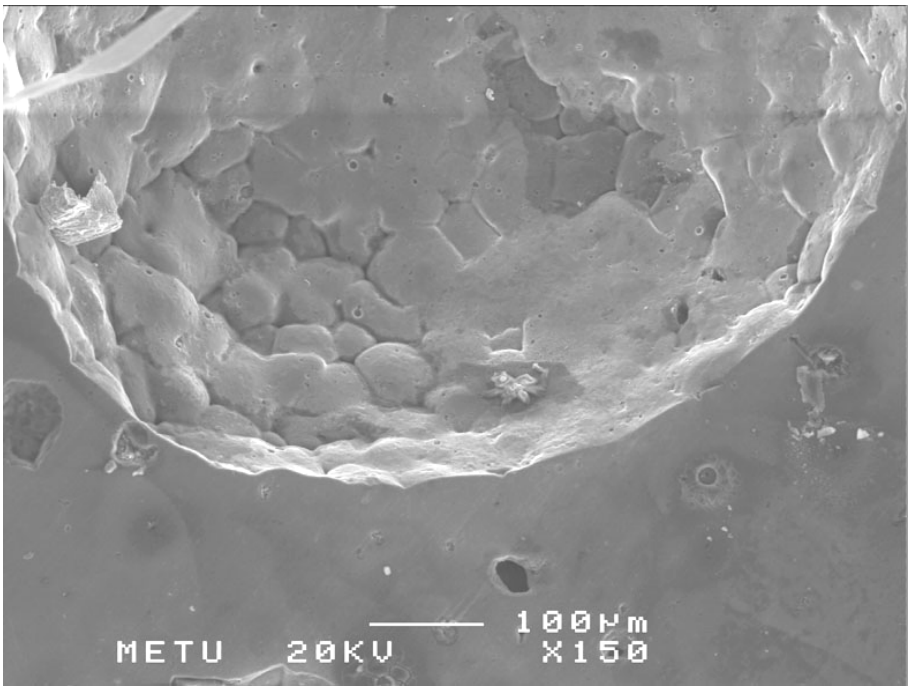

Figure 4.12. Pore structure in Al foam, (Al-8% Al_2O_3-fineTiH_2, 835°C)

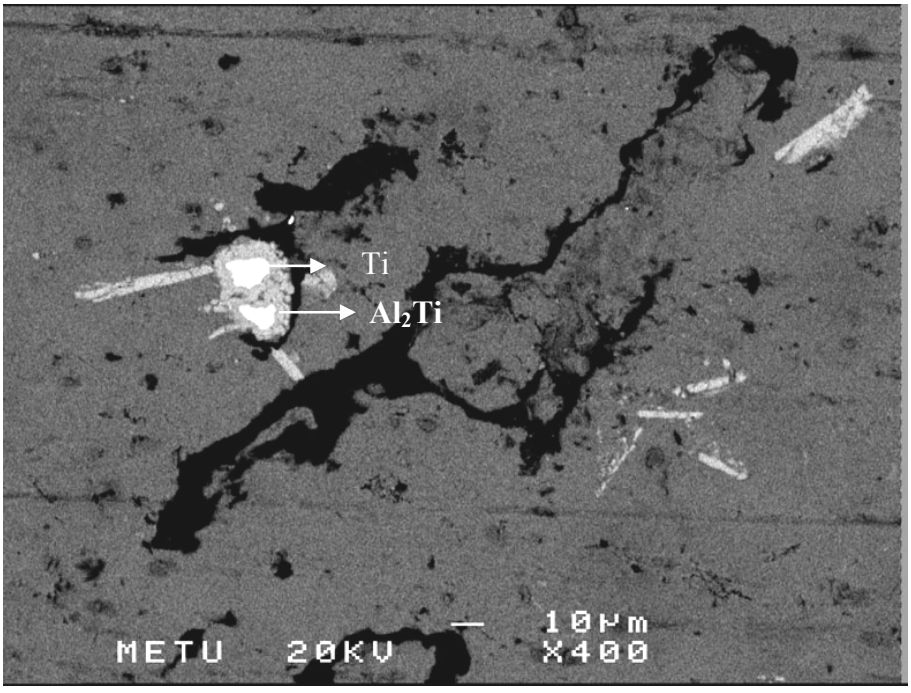

Figure 4.13. SEM image of a foamed sample, (Al-8% Al_2O_3-fineTiH_2,805°C)

4.3.4. Effect of TiH_2 size on foaming of Al

Amount of foaming obtained in samples in a variety of conditions are given in Fig 4.14- 4.16 in the form of three charts. Datas are also tabulated in Table 4.2 and Table 4.3 for samples with fine and coarse TiH_2 respectively.

The amount of foaming is plotted with respect to foaming temperature in Fig. 4.14. It is seen that while with coarse TiH_2, foaming is quite successful at all foaming temperatures; the same is not true for samples with fine TiH_2. The degree of foaming with fine TiH_2 is not significant at low temperatures. The foaming increases gradually with increase in temperature and the foaming in excess of 100 % or more is achieved at and above 800°C. Thus it can be stated that there is clear evidence that foaming is severely temperature dependant with fine TiH_2

Variation of foaming as a function of solid (Al_2O_3) content is given in Fig. 4.15 The degree of foaming is higher with coarse TiH2 particle. For both systems, there is a slight decrease above 10% solid addition, this is especially more pronounced for fine TiH_2.

Fig 4.16 shows the degree of foaming as a function of the expected viscosity. The expected viscosity was calculated with equations 4.1 and 4.2 given in the previous section. Thus this plot combines both the temperature and the solid fraction effects.

Fig. 4.16 shows that with increased viscosity, there is a decrease in the level of foaming achieved. This is true for both coarse TiH_2 and fine TiH_2. For fine TiH_2 the degree of foaming is reduced with increased viscosity and effectively stops for values above 2.3 mPa.s. With coarse TiH_2 the trend is the same, though the value of critical viscosity appears to be higher than 2.3 mPa.s.

Table 4.2. Experimental conditions and the amount of foaming of the systems with fine TiH_2.

Composition	Viscosity	Temperature (°C)	% vol. Expansion
Pure Al + fine TiH_2	1.80	675	186.176
Pure Al+ fine TiH_2	1.80	675	95.725
Pure Al+ fine TiH_2	1.80	675	82.441
Pure Al+ fine TiH_2	1.80	675	135.408
Pure Al+ fine TiH_2	1.80	675	0
Pure Al+ fine TiH_2	1.80	675	121.544
Al-8vol% Al_2O_3+ fine TiH_2	2.20	690	1.460
Al-8vol% Al_2O_3+ fine TiH_2	2.20	690	59.831
Al-8vol% Al_2O_3+ fine TiH_2	2.20	690	77.537
Al-12vol% Al_2O_3+ fine TiH_2	2.42	690	0
Al-12vol% Al_2O_3+ fine TiH_2	2.42	690	32.298
Pure Al+ fine TiH_2	1.70	700	193.340
Pure Al+ fine TiH_2	1.70	700	0
Pure Al+ fine TiH_2	1.70	700	47.554
Pure Al+ fine TiH_2	1.70	700	158.975
Pure Al+ fine TiH_2	1.70	700	146.867
Al-10vol% Al_2O_3+ fine TiH_2	2.32	700	42.603
Al-10vol% Al_2O_3+ fine TiH_2	2.32	700	46.847
Al-8vol% Al_2O_3+ fine TiH_2	2.10	720	160.307
Al-8vol% Al_2O_3+ fine TiH_2	2.10	720	167.1784
Al-12vol% Al_2O_3	2.32	740	36.079
Al-12vol% Al_2O_3+ fine TiH_2	2.32	740	46.930
Al-12vol% Al_2O_3+ fine TiH_2	2.20	770	23.221
Al-12vol% Al_2O_3+ fine TiH_2	2.20	770	80.883
Al-8vol% Al_2O_3+ fine TiH_2	1.80	805	107.185
Al-8vol% Al_2O_3+ fine TiH_2	1.80	805	93.533
Al-8vol% Al_2O_3+ fine TiH_2	1.70	835	167.412

Table 4.2. Experimental conditions and the amount of foaming of the systems with coarse TiH_2.

Composition	Viscosity	Temperature (°C)	% vol. Expansion
Pure Al + Coarse TiH_2	1.80	675	250.21
Pure Al+ Coarse TiH_2	1.80	675	163.19
Al-10vol% Al_2O_3+ Coarse TiH_2	2.57	680	96.999
Al-8vol% Al_2O_3+ Coarse TiH_2	2.20	690	104.07
Al-8vol% Al_2O_3+ Coarse TiH_2	2.20	690	189.55
Al-12vol% Al_2O_3+ Coarse TiH_2	2.42	690	0
Al-12vol% Al_2O_3+ Coarse TiH_2	2.42	690	106.77
Pure Al+ Coarse TiH_2	1.70	700	118.88
Pure Al+ Coarse TiH_2	1.70	700	195.96
Al-10vol% Al_2O_3+ Coarse TiH_2	2.32	700	160.99
Al-10vol% Al_2O_3	2.32	700	143.96
Al-8vol% Al_2O_3+ Coarse TiH_2	2.10	720	87.732
Al-8vol% Al_2O_3+ Coarse TiH_2	2.10	720	541.05
Al-12vol% Al_2O_3+ Coarse TiH_2	2.57	720	91.411
Al-12vol% Al_2O_3+ Coarse TiH_2	2.57	720	102.76
Al-14vol% Al_2O_3+ Coarse TiH_2	2.42	735	34.822
Al-14vol% Al_2O_3+ Coarse TiH_2	2.42	735	151.82
Al-12vol% Al_2O_3+ Coarse TiH_2	2.32	740	148.85
Al-12vol% Al_2O_3+ Coarse TiH_2	2.32	740	133.31
Al-12vol% Al_2O_3+ Coarse TiH_2	2.32	740	148.85
Al-12vol% Al_2O_3+ Coarse TiH_2	2.32	740	133.31
Al-12vol% Al_2O_3+ Coarse TiH_2	2.20	770	0
Al-12vol% Al_2O_3+ Coarse TiH_2	2.20	770	145.14
Al-12vol% Al_2O_3+ Coarse TiH_2	2.20	770	0
Al-12vol% Al_2O_3+ Coarse TiH_2	2.20	770	145.14
Al-8vol% Al_2O_3+ Coarse TiH_2	1.80	805	175.17
Al-8vol% Al_2O_3+ Coarse TiH_2	1.80	805	106.43
Al-8vol% Al_2O_3+ Coarse TiH_2	1.70	835	101.81
Al-8vol% Al_2O_3+ Coarse TiH_2	1.70	835	181.81

4.3.4.1 Minimum critical particle size

Following Tan, 2003, the foaming occurs due to the decomposition of TiH_2. Hydrogen gas initiates a pore around a hydride particle and this pore expands by displacing the liquid aluminum. According to the ideal gas law, the pressure inside the pore, P_{in},

$$P_{in}V = n_{H2} R T \quad \textbf{(4.3)}$$

where V is the volume of the pore, n_{H2} mole number of H_2 evolved, R is the general gas constant and T is the temperature in degrees Kelvin.

If the pore is assumed to be spherical with r radii, it is thought that the r is equal to the size of TiH_2 at the beginning of the process.

$$V = \frac{4}{3}\pi r^3 \quad \textbf{(4.4)}$$

From the results reported above, it appears that the size of foaming agent appears to produce quite pronounced effects on the various aspects of foaming. Of these, perhaps the most important aspect is that reported in Fig. 4.14. Here it appears that foaming with fine TiH_2 the use of much higher foaming temperature is a necessity. This aspect is evaluated further by following the notion proposed by Tan that, there is a critical value for foaming agent which must be exceeded for successful foaming.

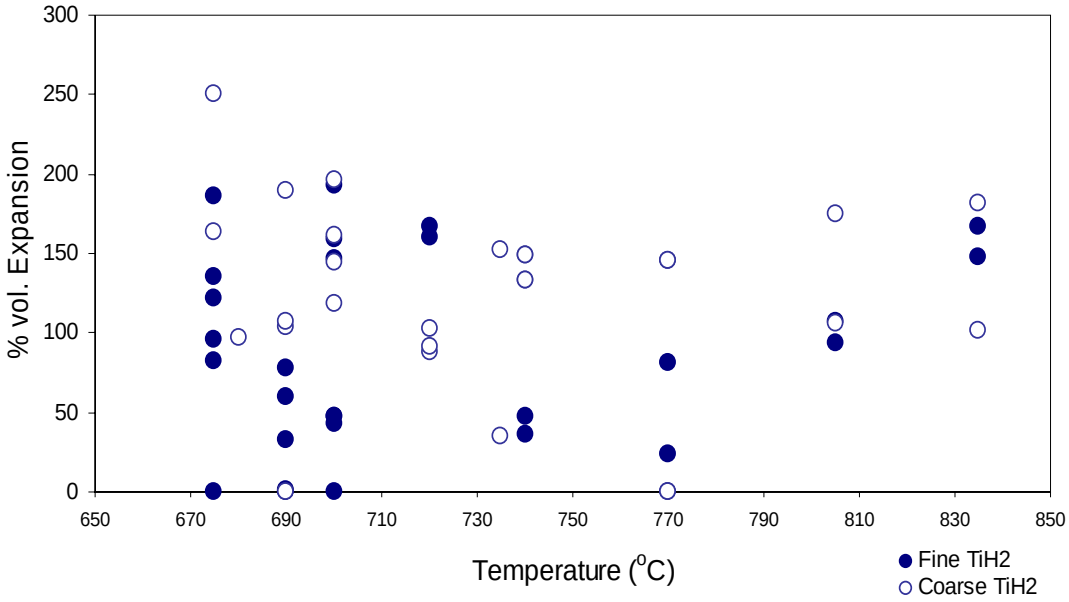

Figure 4.14. Variation of the amount of foaming with respect to temperature

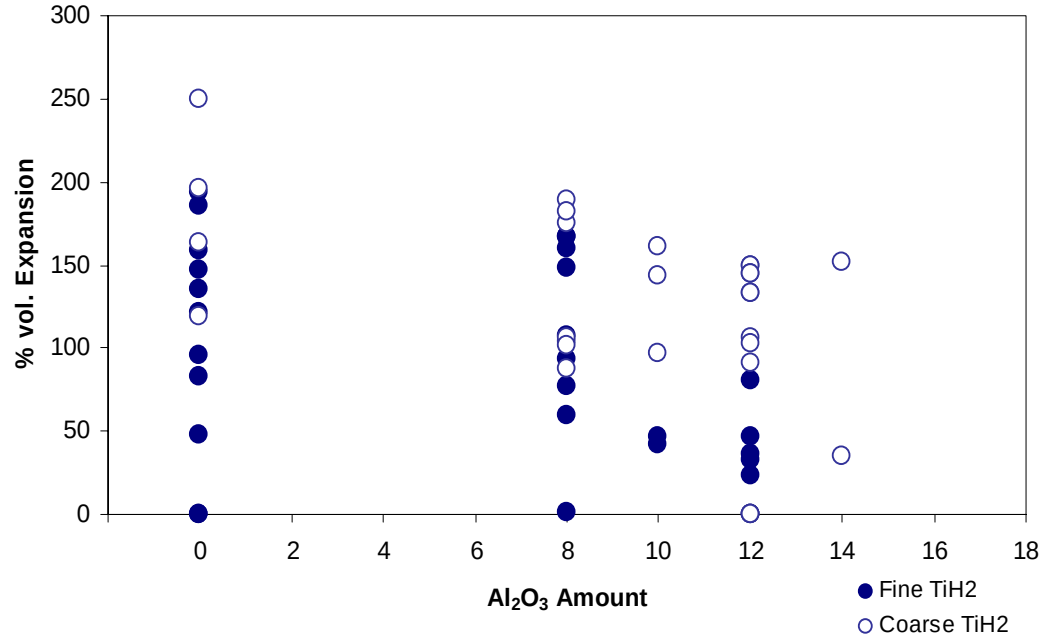

Figure 4.15. Variation of the amount of foaming with respect to Al_2O_3 amount.

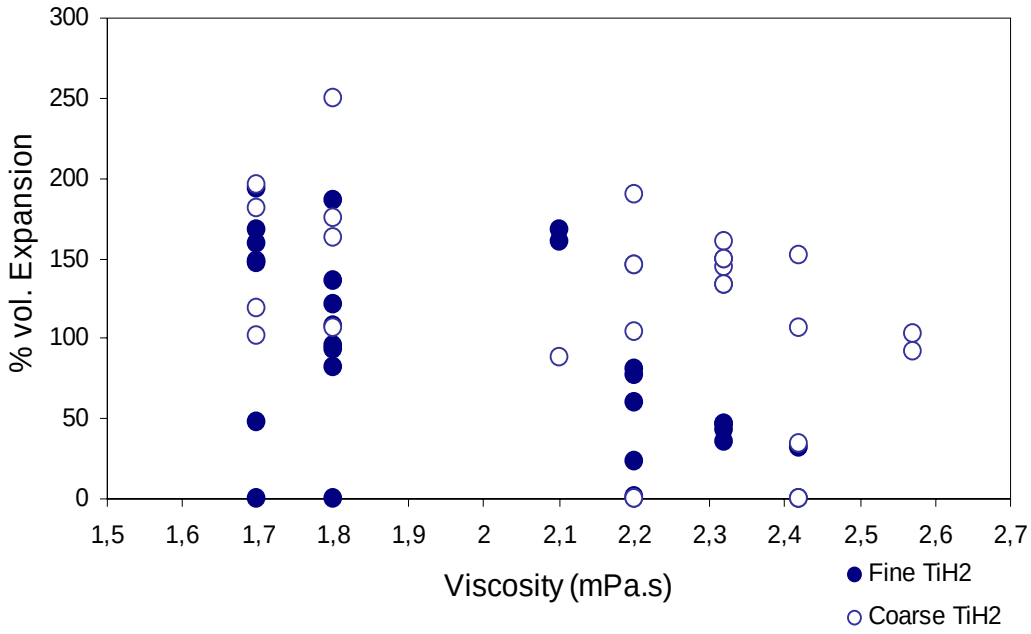

Figure 4.16. Variation of the amount of foaming with respect to viscosity.

If equation 4.3 and 4.4 are combined, internal pressure inside the pore,

$$P_{in} = \frac{3n_2 RT}{4\pi r^3} \qquad \textbf{(4.5)}$$

At the beginning of the process, P_{in} is smaller but as the decomposition proceeds to evolve more hydrogen, and pressure increases.

Decomposition process proceeds at low pressure however as the evolved hydrogen increases pressure increases and when the reaction reaches an equilibrium, the reaction stops. According to Mueller (1968), equilibrium pressure of TiH_2, Pe_q;

$$\ln P_{eq} = \frac{-19821}{T} + 21{,}671 \qquad \textbf{(4.6)}$$

where T is the reaction temperature.

The pore to expand, internal pressure of the pore should be larger than external pressure.

External pressure acting on the pore equals to the sum of the hydrostatic pressure of liquid aluminium (P_h), atmospheric pressure (P_a) and pressure due to surface tension between liquid aluminium (Ps) and the pore, i.e

$$P_{ext} = P_h + P_a + P_s \quad \textbf{(4.7)}$$

If hydrostatic pressure (since the samples are small) and atmospheric pressure are neglected, external pressure, P_{ext}, becomes,

$$P_{ext} = P_s = \frac{2\gamma}{r} \quad \textbf{(4.8)}$$

Here γ is the surface tension and r is the radius of the pore.

Therefore external pressure of the pore is determined by the surface tension of aluminium. Surface tension of aluminium and its variation with temperature is given by Saravanan et al.,2001;

$$\gamma = -0{,}1527 \cdot T + 1032{,}2 \quad \textbf{(4.9)}$$

To expand the pore, the required condition is that $P_{in} > P_{ext}$. Maximum internal pressure can be equal to equilibrium pressure.

$$P_{eq} >= P_{ext} \quad \textbf{(4.10)}$$

P_{eq} and P_{ext} values could be calculated by using 4.6 and 4.8 respectively for different pore sizes at a given temperature. Figure 4.17 shows the variation of these parameters at 750°C. It is seen that the external pressure decreases with increasing pore size. Equilibrium pressure on the other hand is independent of pore size.

It is seen that P_{eq} intersects with P_{ext} at a point designated as d_{cr}. d_{cr} shows the minimum critical particle size required for foaming. In other words, if the size of

foaming agent is above this value, foaming takes place. If the size of foaming agent is below this value, on the other hand foaming does not occur since external pressure is higher than the internal one.

The evaluation given in Fig 4.17 that refer to 750°C is repeated at other temperatures. The results are given in Fig. 4.18, which shows the value of critical particle size for foaming agent as a function of temperature.

At 675°C, the critrical size of TiH_2 is d_{cr} = 30 μm. This value is reduced to a few microns at temperatures above 800°C. In other words, in systems with 30 μm or above TiH_2 particles foaming is expected at all temperatures but for the systems using a few microns of TiH_2 the use of temperatures higher than 800°C is requirement. This prediction is in agreement with the observation reported in Fig 4.14.

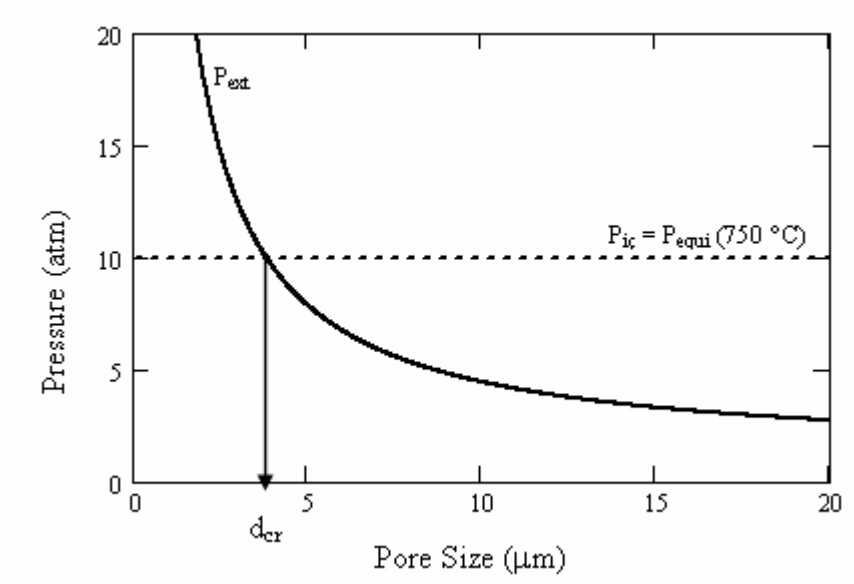

Figure 4.17. Variation of external pressure with pore size is shown at 750 °C. Intersection point of external pressure with equilibrium pressure gives the minimum critical particle size.

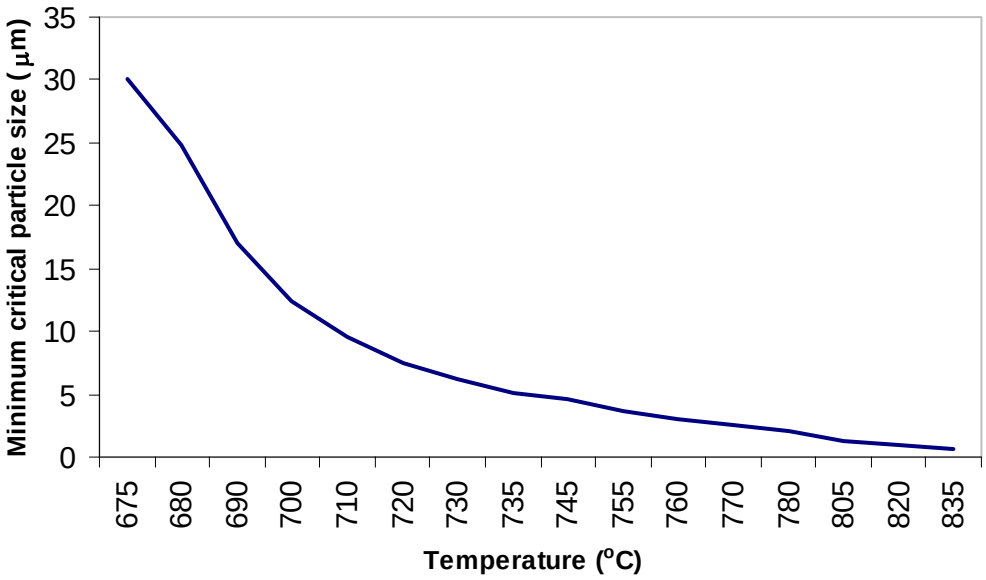

Figure 4.18. Variation of the minimum critical particle size with temperature. Critical value required for foaming decreases with increasing temperature.

CHAPTER V

CONCLUSION

Aluminium foams are produced via powder metallurgy with the use of fine (8,5 μm) and coarse (27,5 μm) TiH_2. Al_2O_3 is used in amounts ranging from 0 to 14 vol %. to adjust the viscosity of the melt. Foaming experiments were carried out at various temperatures between 675- 840°C.

The study showed that the foaming agent TiH_2 size is influential in foaming process. It is found that with fine TiH_2 the use of 800°C or higher temperatures is required for successful foaming. It is also found that viscosity of 2.3 mPa.s is a limiting value for successful foaming with fine TiH_2. This limiting value seems to increase with increase in TiH_2 particle size.

It is shown that temperature dependence of foaming as observed with fine TiH_2 size can be explained based on a notion of the critical size for foaming agent. This size as calculated in this study ranges from 30 μm at 675°C to 0,7 μm at 835°C.

REFERENCES

Arefmanesh A., Advani S. G., Michaelides E. E., Polymer engineering and science, vol 30, no 20, (1990), 1330-1337.

Andrade, E. N. Phil. Mag., (1934), vol.17, 698.

Amon M., Denson C. D., Polymer engineering and science, vol 24, no 13, (1984), 1026-1034.

Banhart J., Europhysics news, 30, 17, (1999)

Banhart J., JOM, 52, 12, (2000), 22-27

Battezzati L., Greer A.L., Acta Materialia, vol.37, No.7, (1989), 1791-1802.

Benning C. J., Plastic foams, vol 1, (1969), John Wiley and Sons Inc.

Bretsznajder S., 1971,' Prediction of Transport and Other Physical Properties of Fluids ', International Series of Monog. in Chem. Eng. Vol. 11, (Pergamon Press, New York).

Colton J. S., Suh N. P., Polymer engineering and science, vol 27, no 7, (1987), 500-503.

Davies G.J., Zhen S., Journal of Materials Science, 18, (1983), 1899-1911

Degischer H. P., Kristz B., (2002), Wiley-vch.

Deqing W., Ziyuan S., Materials Science and Engineering, A361, (2003), 45-49.

Edwards S. F., Pithia K. D., Physica A, 215, (1995), 270-276.

Frye G. C., Berg J. C., Journal of Colloid and Interface Science, vol 127, No:1, (1989), 222-238.

Frye G. C., Berg J. C., Journal of Colloid and Interface Science, vol 130, No:1, (1989), 54-59.

Fuganti A., Lorenzi L., Advanced Engineering materials, 2, 4, (2000), 200-204.

Fusheng H., Jianning W., Hefa C., Junchang G., Journal of materials processing technology, 138, (2003), 505-507.

Garrett P. R., Journal of Colloid and Interface Science, vol 69, No:1, (1979), 107-121.
Gergely V., Clyne B., Advanced Engineering Materials, 2, No.4, (2000), 175-178.

Gibson L.J., Ashby M.F., 1997, ' Cellular Solids, 2nd Edition ', (Cambridge University Press)

Hirai, M ISIJ, vol.33, (1993), 281-258.

Hobbs S. Y., Polymer engineering and science, vol 16, no 4, (1976), 270-175.

Hudales J.B.M., Stein H. N., Journal of Colloid and Interface Science, vol 140, No:2, (1990), 307-313.

Jalmes A. S., Langevin D., Journal of Physics: Condensed Matter, 14, (2002), 9397-9412.

Kaptay G. Colloids and Surfaces A: Physicochemical and Engineering Aspects, vol 230, 1-3, (2003), 67-80.

Kennedy A. R. Materials Science and engineering, A357, (2003), 258-263

Klempner D., Frisch K. C., Handbook of polymeric foams and foam technology, 1991, (Oxford University Press).

Koehler S. A., Stone H. A., Brenner M. P., Eggers J., Physical Review, vol 58, No:2, (1998) 2097-2106.

Körner C., Singer R. F., Advanced Engineering materials, 2, 4, (2000), 159-165.

Leitlmeier D., Degischer H.P., Flankl H.J., Advanced Engineering Materials, 4, No.10, (2002), 735-740.

Lillico D. A., Babchin A. J., Jossy W. E., Sawatzky R. P., Yuan J. K., Colloids and Surfaces A: Physicochemical and Engineering Aspects, 192, (2001), 25–38.

Miyoshi T., Itoh M., Akiyama S., Kitahara A., Advanced Engineering Materials, 2, No.4, (2000), 179-183.

Mueller W.M., Blackkedge J.P., Libowitz G.G., (1968), 'Metal Hydrides', (Academy Press Inc., London).

Park S., Hur B., Kim S., Ahn D., Ha D., 2002, in ' 65th World Foundry Congress Proceedings ‘, 515-522.

Saravanan et al.,Scripta Mater., 44,(2001), 965-970

Shafi M. A., Joshi K., Flumerfelt R. W., Chemical engineering science, vol 52, no 4,

(1997), 635-644.

Shafi M. A., Flumerfelt R. W., Chemical Engineering Science, vol 52, no 4, (1997), 627-633.

Song Z. L., Ma L. Q., Wu Z. J., He D. P., Journal of Materials Science, 35, (2000), 15-20.

Stone H. A., Koehler S. A., Hilgenfeldt S., Durand M., Journal of physics: Condensed Matter, 15, (2003), 283-290.

Tang F. Q, Xiao Z., Tang Jı-An., Jiang L., Journal of Colloid and Interface Science, vol 131, No:2, (1989), 498-502.

Tan S., Ms.Thesis, Middle East Technical University, Metallurgical and Materials Engineering, (2003).

Wübben Th., Stanzick H., Banhart J., Odenbach S., Journal of Physics C: Solid State Physics (2002),.

Yang C. C., Nakae H., Journal of Alloys and Compounds, 313, (2000), 188-191.